

Mirror Technology Development Roadmap for the International X-ray Observatory (IXO)

**Prepared by
The Glass Mirror Technology Development Team**

Goddard Space Flight Center
Marshall Space Flight Center
Smithsonian Astrophysical Observatory

5 May 2009

Table of Contents

1	Introduction.....	10
2	Requirements	11
3	Mirror Segment Fabrication.....	14
3.1	Forming Mandrels	14
3.2	Slumping.....	16
3.2.1	Boron Nitride Release Layer.....	18
3.2.2	Platinum and Platinum-Gold Alloys Release Layer.....	19
3.3	Post-Slumping Cutting.....	20
3.4	Coating.....	21
3.5	Metrology.....	23
4	Mounting, Alignment, and Bonding.....	27
4.1	Passive Approach	28
4.2	Active Approach.....	34
5	Mirror Module Design and Construction	40
5.1	Preliminary Design.....	40
5.2	Development Testing.....	41
5.3	Selection of Alignment Approach.....	42
5.4	Detailed design and analysis	43
5.5	Fabrication and Testing	43
5.6	Large Segment Alignment and Bonding Demonstration Testing	44
6	Appendix.....	46
6.1	Mirror Segment Description	46

Summary

The challenge of the X-ray optics for the International X-ray Observatory mission lies in meeting four requirements simultaneously: (1) angular resolution, (2) effective area, (3) mass, and (4) production schedule. Given its 5 arcsec observatory level requirement, IXO requires a 4 arcsec flight mirror assembly (FMA). The FMA, which consists of 60 modules, in turn requires 3.8 arcsec modules. This document is a roadmap for developing a mirror technology that by heritage has already met three of the four requirements: effective area, mass, and production schedule. Our development effort focuses on improving this technology to meet the angular resolution requirement. Specifically, the objective of this technology development program is to develop two techniques that, when appropriately combined and engineered, can meet the angular resolution requirement:

1. a glass slumping technique that can make mirror segments with a mass areal density less than 1 kg/m^2 ;
2. a handling technique that is capable of aligning and bonding these lightweight mirror segments with the required optical precision.

This roadmap takes the technology to TRL-6 by the end of 2011. We have divided the development work into several small pieces that can be pursued and completed in parallel at different institutions. Then they will be brought together to manufacture mirror segments and integrate these mirror segments into a “flight-like” mirror module. This mirror module will be subject to a complete battery of tests: X-ray performance, vibration, acoustic, and thermal-vacuum, to demonstrate TRL-6.

Table 1 shows the definitions of TRL-4, 5, and 6 interpreted for this specific technology. Table 2 shows the several components whose completion will ensure the success of this development program. Table 3 is the development schedule.

Table 1. Definitions of TRL-4, TRL-5, and TRL-6 for this technology development. These definitions are used to gauge development status.

	Number of Mirror Pairs Aligned and Bonded	Housing Structure Fidelity	Angular Resolution of X-ray Images	Environment Tests
TRL-4	1	Housing structure simulator; Not lightweighted; May not be suitable to withstand vibration testing	~15 arcsecs HPD (two reflections) at one or more energies	Different tests may use different individual mirror segments; Pass tests separately
TRL-5	2 or 3	Housing simulator; Not lightweighted; Able to withstand vibration testing	10 arcsec HPD (two reflections), at one or more energies	Different tests may use different individual mirror segments; May pass tests separately; Complete set of tests to demonstrate agreement between model and data
TRL-6	3	“Flight-like;” Fully lightweighted and modeled; Able to withstand all tests: thermal-vacuum, vibro-acoustic, and X-ray	3.8 arcsec HPD (two reflections), at several energies spanning the IXO band of 0.1 to 7 keV	Comprehensive tests: X-ray, vibration, acoustic, thermal-vacuum, and X-ray test again to verify performance; Complete documentation

Table 2. Summary of the mirror technology development effort. Each row represents an area of development. For the most part, each area can be developed in parallel with others, enabling efficient utilization of time and money.

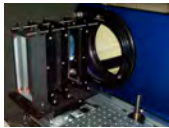
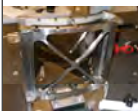
Technology Component Description		Graphic Representation	Error Budget Allocation			Comment		
			Contribution to Angular Resolution (arcsec)	Cumulative Angular Resolution (arcsec)				
				One Reflection	Two Reflections			
Mirror Segment Fabrication (Section 3)	Making Forming Mandrels (Section 3.1)	Fabrication of mandrels for developing the glass slumping process		1.5	1.5	2.1	Not part of technology development per se, but important for enabling the mirror technology development	
	Slumping (Section 3.2)	Replication of the mandrel figure to a glass sheet through the thermal forming process		1.6	2.2	3.1		
	Cutting (Section 3.3)	Cutting the glass substrate to dimension so that it mechanically fits in housing; Leaving smooth and fracture-free edges		0.0	2.2	3.1	Areas of development include: (1) improvement of mandrel release layer smoothness; (2) reduction and/or elimination of iridium coating stress; (3) Understanding of metrology mount distortion of mirror segments to be able to derive the mirror segment's intrinsic figure	
	Coating (Section 3.4)	Sputter coating of substrate surface with 15nm of iridium to enhance x-ray reflectivity and maximize effective area		0.8	2.3	3.3		
	Measuring (Section 3.5)	Complete measurement of the optical figure of the finished mirror segment: (1) feedback to the fabrication process, (2) benchmark for subsequent mounting, aligning, and bonding process		0.0	2.3	3.3		
Mounting, Aligning, and Bonding (Section 4)	Mounting	Temporarily bonding or holding the flexible mirror segment to a structure so that it can be manipulated for alignment and bonding	Passive Approach (Section 4.1) 	Active Approach (Section 4.2) 	0.1	2.3		3.3
		Adjustment of the orientation and/or figure of the mirror segment to achieve optical alignment with other mirror segments			0.2	2.3		3.3
	Bonding	Permanent bonding of mirror segments to housing to preserve alignment and to withstand launch loads			0.9	2.5	3.6	
Module Design and Construction (Section 5)	Design and creation of thermal and mechanical and acoustical environments for mirror segments; Analysis and understanding and elimination/minimization of optical figure distortion; Lightweighting design to meet mass requirement		1.0	2.7	3.8	Finished module will have at least three pairs of optically qualified mirror segments and mass dummies to simulate loads; Will undergo a complete battery of tests to qualify for TRL-6		

Table 3. Top Level Schedule of the Technology Development Program - Page 1 of 4

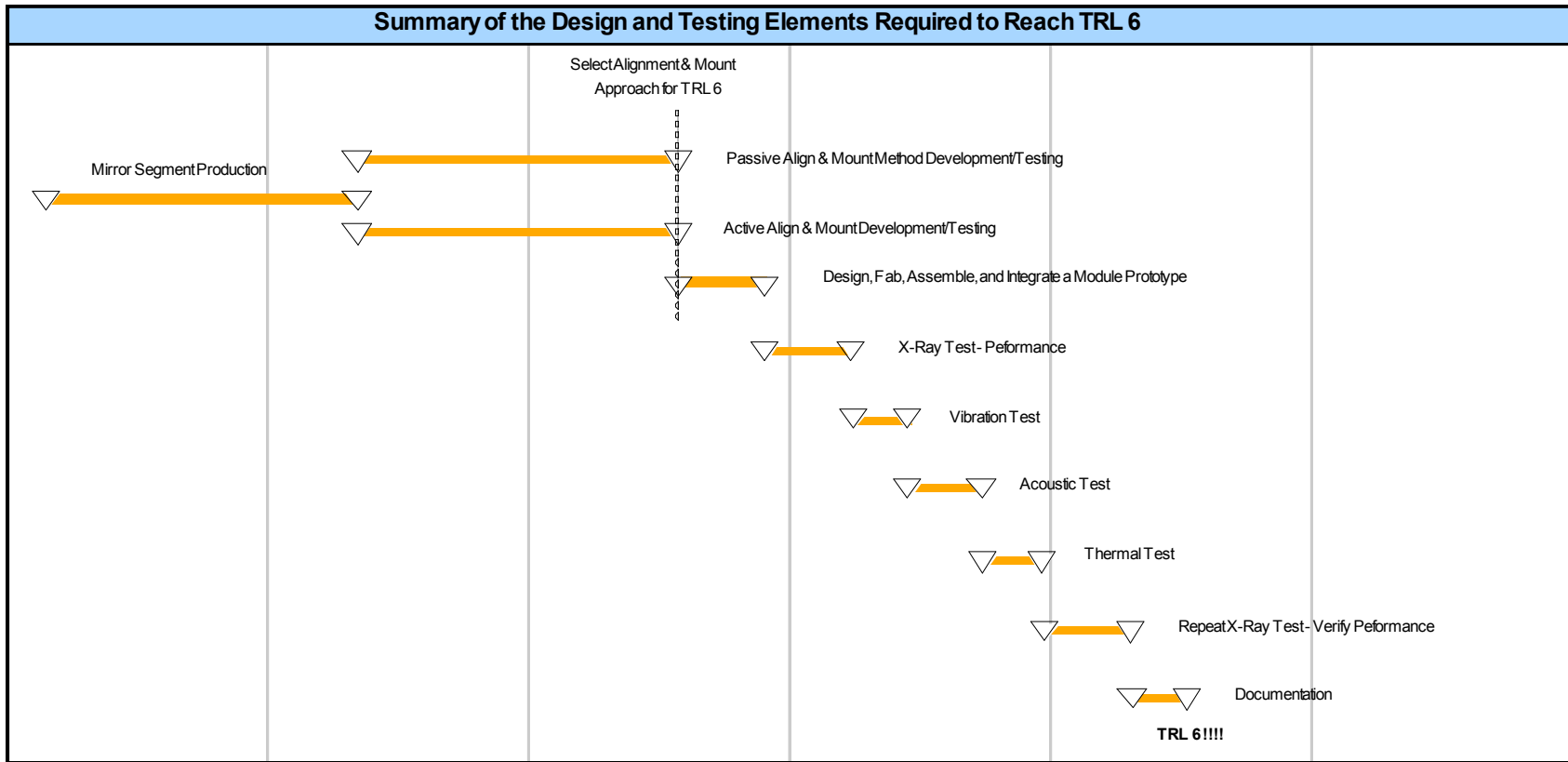


Table 3. Top Level Schedule of the Technology Development Program - Page 2 of 4

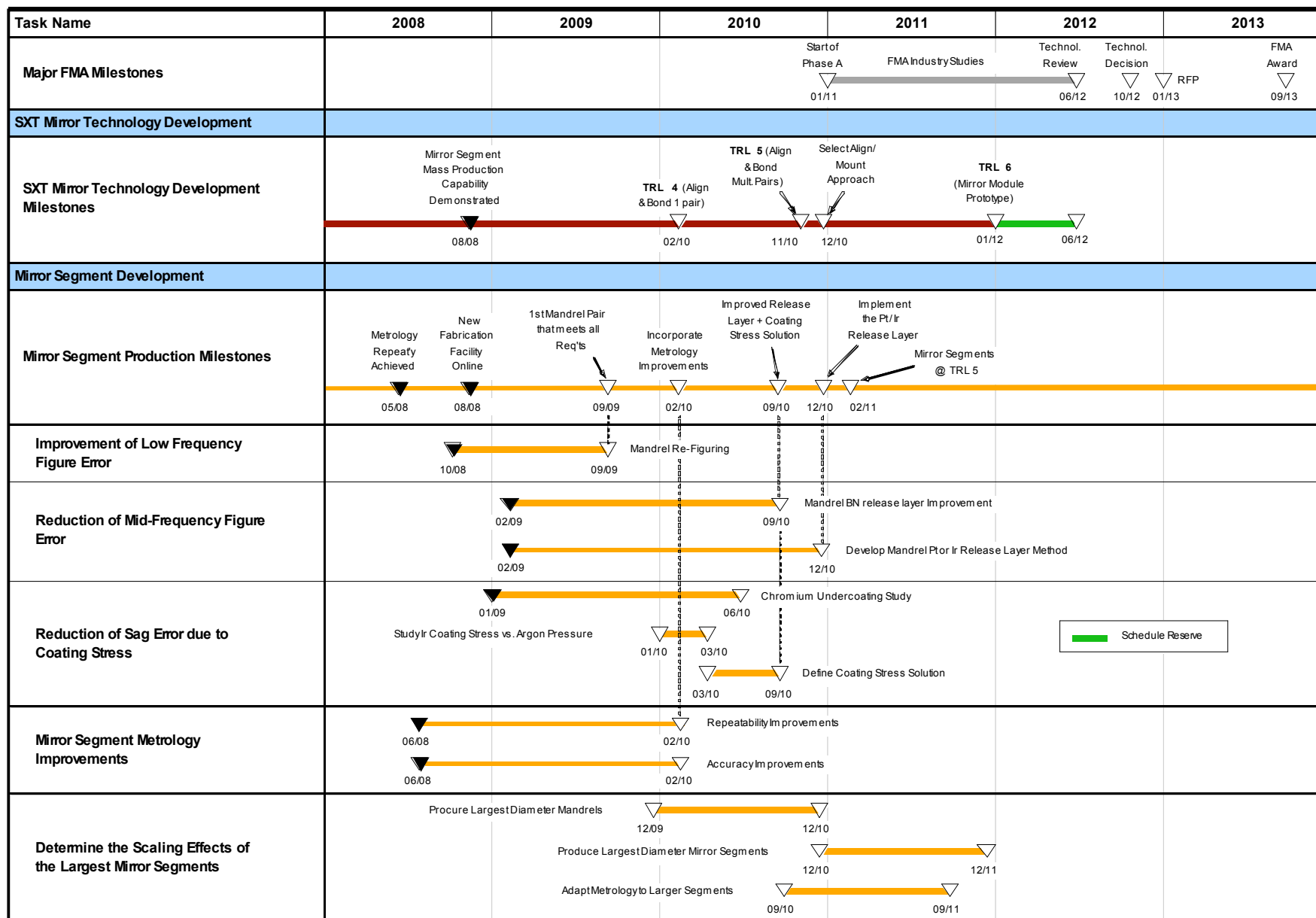
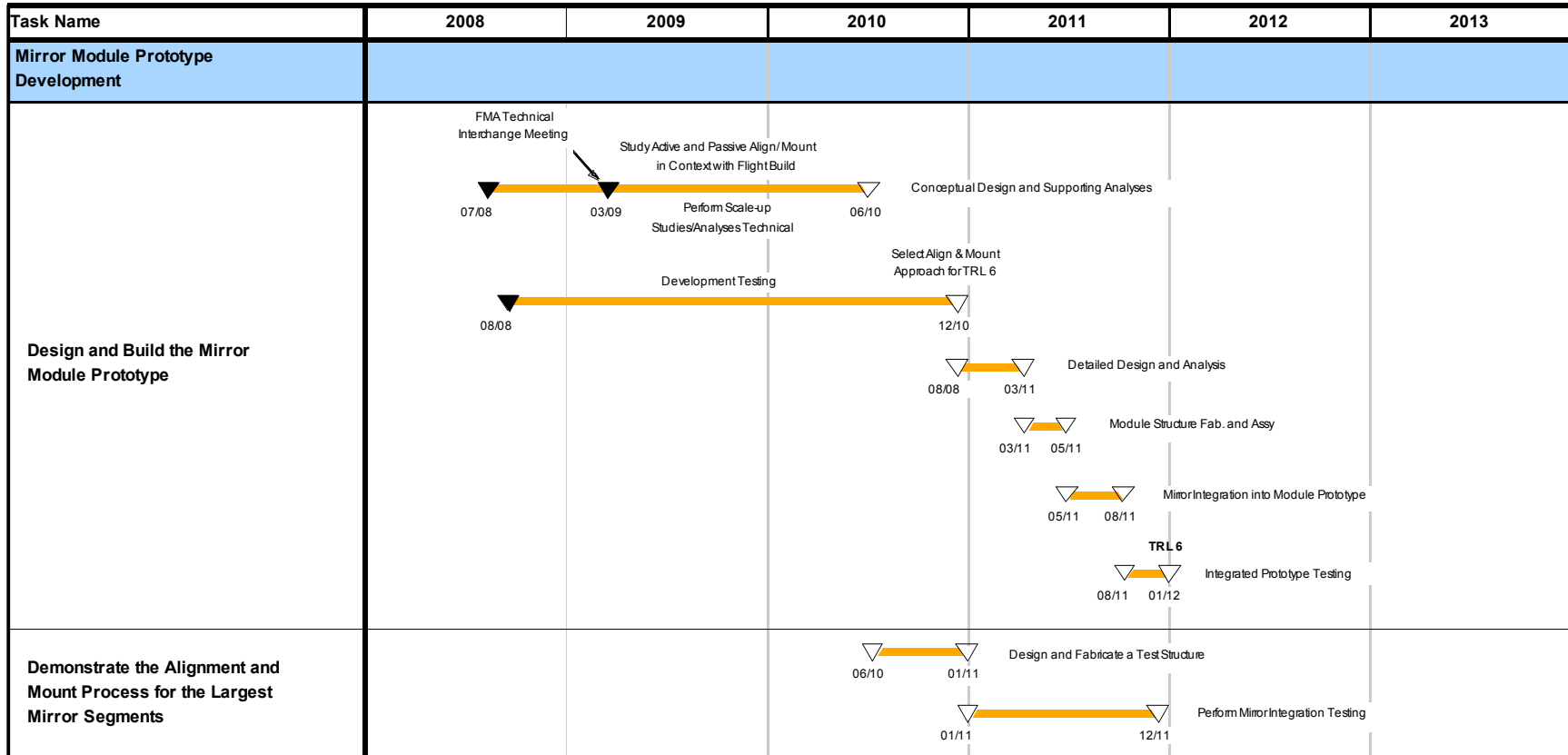


Table 3. Top Level Schedule of the Technology Development Program - Page 3 of 4

Task Name	2008	2009	2010	2011	2012	2013
Mirror Segment Alignment and Mount						
Passive Technology Approach						
Temporary Mount - Bond an Individual Mirror Segment to a Transfer Mount without Distortion	Temp. Mount Repeafy 04/08 06/08	4-PtMount X-Ray Test 11/08	8-PtMount X-Ray Test 10/09 12/09	[Strongback]	TRL 6	
Permanent Mount - Bond an Individual Mirror Segment to a Structure without Distortion		4-PtBond X-Ray Test 10/08 02/09	8-PtBond X-Ray Test 11/09 12/09	[Mirror Bonding Strongback]		
Align and Bond a Mirror Pair onto a Structure		4-PtBond X-Ray Test 05/09	8-PtBond X-Ray Test 07/09 12/09	TRL 4 [Mirror Housing Simulator]		
Align and Bond \geq Two Mirror Pairs onto a Structure		4-PtBond X-Ray Test 08/09	8-PtBond X-Ray Test 01/10 07/10	Environmental Testing 09/10	X-Ray Test 11/10	TRL 5 [Mirror Housing Simulator]
Align and Bond \geq Two Mirror Pairs into an Engineering Model			8-PtBond X-Ray Test 07/10	Environmental Testing 02/11 04/11	X-Ray Test 06/11	[Mini-Module]
Active Technology Approach						
Adjust the Focal Length of a Single Mirror Segment and Bond to a Structure	07/08 [OAP-2]					
Align and Bond a Mirror Pair onto a Structure	07/08	TRL 4	11/09	[OAP-2 / OAP-3]		
Align and Bond \geq Two Mirror Pairs onto a Structure		X-Ray Test 12/09	Environmental Testing 03/10 04/10	X-Ray Test 06/10	TRL 5 [OAP-4]	

Table 3. Top Level Schedule of the Technology Development Program - Page 4 of 4



1 Introduction

The International X-ray Observatory will have an angular resolution of 5 arcsecs or better in the energy band of 0.1 to 7 keV. IXO systems level error budget allocates 4 arcsecs HPD (half-power diameter) error to the Flight Mirror Assembly (FMA) and the remaining error to the observatory systems level. As such the FMA must meet the following four requirements:

1. Angular resolution: 4 arcsecs HPD as built and tested on the ground
2. Effective area: 3 m² at 1.25 keV
3. Total mass less than 1,800 kg
4. Manufacture schedule that can accommodate the overall project schedule.

The baseline design, which meets these four requirements, divides the FMA into 60 modules: 12 identical inner modules, 24 identical middle modules, and 24 identical outer modules, as shown in Figure 1. Each mirror module contains between 143 (inner) and 103 (outer) pairs of parabolic and hyperbolic mirror segments. In this baseline design, approximately half of the total FMA mass is in the mirror segments and the other half in the module housings and the mechanical structures supporting the modules.

The baseline design imposes the following requirements on the mirror segments:

1. They must have an areal density of 1 kg/m² or less;
2. They must not be thicker than about 0.4mm; and
3. They must meet optical figure quality and mechanical dimension requirements and must be precisely aligned and bonded into the module housing.

Integrating the 60 modules together to form the FMA requires good planning and careful engineering, but it is substantially similar to other tasks that have been done for other missions in the past. It requires no new technology. As such the only unique and new areas of technology required for IXO are:

1. Fabrication of the mirror segments, and
2. The precision mounting, alignment, and permanent bonding of these mirror segments into a module housing.

This technology development effort focuses on these two areas. We slump commercially available glass sheets to make mirror segments. It is a replication technique and, by design and heritage (NuSTAR mission), amenable to mass production. The challenge is the imparting of precise parabolic or hyperbolic figures to the flat glass sheets. In the area

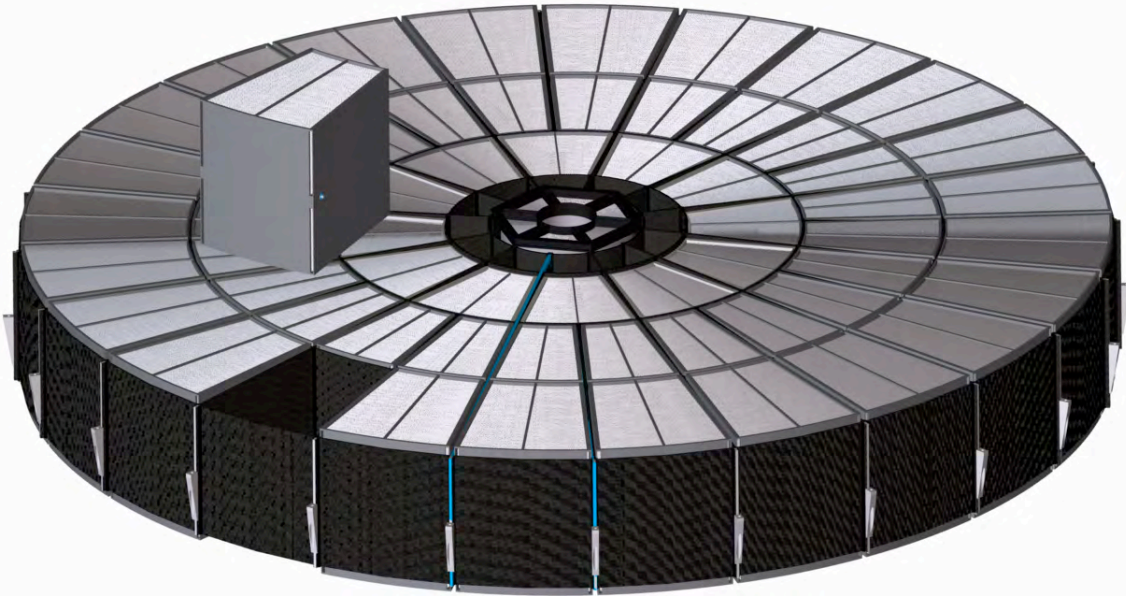


Figure 1. The baseline design FMA. It has a total of 60 modules integrated to an overall support structure. The outermost shell has a diameter of 3.2m. The focal length is 20m.

of mounting, alignment and bonding, the challenge is to overcome the relative flexibility of these mirror segments and over-constrain them without degrading their optical figures. This approach is consistent with the program requirements. This roadmap focuses on surmounting the few remaining technical difficulties necessary to achieve performance requirements.

Table 2 is a top-level summary of the components of this technology development. Sections 2 through 5 elaborate on this summary, both in terms of what has been accomplished and what needs to be accomplished to reach TRL-6.

2 Requirements

This mirror technology development program is creating and maturing techniques of fabrication, mounting, alignment and bonding of glass mirror segments. The result of this technology development program is two-fold:

1. The design and construction of one or more mirror modules to demonstrate the validity of these techniques, showing this technology at TRL-6 level (see detailed definition below);
2. Documentation that describes the techniques so that industrial contractors could employ them to plan and construct facilities for the manufacture of the flight mirror assembly (FMA).

In this specific context, reaching TRL-6 means that we will have developed and validated the necessary techniques for designing and constructing a flight-like mirror module that passes the following sequence of tests:

1. Full illumination X-ray tests at energies ranging from 0.1 keV to 7 keV, meeting both angular resolution and effective area requirements;
2. Vibro-acoustic tests at qualification levels, ensuring mirror segment to withstand the launch environment;
3. Thermal vacuum tests, ensuring mechanical and performance stability over time and in varying environments; and
4. A second set of full illumination X-ray tests to verify that the mirror module has not sustained any damage or permanent performance degradation as a result of the previous tests.

In this specific context, “flight-like” means the following:

1. The mechanical structure of the module meets the mass requirement and is constructed of a material that could be used for the flight mirror assembly;
2. Mirror segments are aligned and bonded using the same process as can be used for flight mirror segments; and
3. The mirror segments will be fabricated using the same process as will be used for the flight mirror segments.

The focal length and actual dimensions of the module may or may not be exactly the same as a flight module, depending on availability of forming mandrels that determine the size of the mirror segments and the module. For the same reason, there will be some segments (at least three pairs) that meet required optical quality, while others will be mass dummies to simulate mechanical loads.

Table 4 is a tentative error budget to guide this technology development effort. Each line represents a specific requirement that is operationally defined and will be operationally verified with specific optical and/or X-ray measurement. As the effort progresses, these numbers will be adjusted if and when necessary.

The following sections of this document describe the issues that need to be addressed and our approaches to address them for this technology to reach TRL-6 by the end of 2011.

Table 4. High level error budget that guides the mirror technology development.

	HPD (arcsec)	Note
Forming Mandrel	1.5 (one reflection)	Based on optical metrology using interferometers and coordinate measuring machines (CMM), assuming the other mandrel being mathematically perfect
Individual Free Standing Mirror Segment	2.3 (one reflection)	Based on optical metrology assuming the other mirror segment being mathematically perfect; The contribution of the mirror fabrication process to this HPD is 1.7 arcsecs
Individual Bonded Mirror Segment	2.4 (one reflection)	Based on optical metrology assuming the other mirror being mathematically perfect; The process of mounting and bonding contributes 0.7 arcsecs to this HPD
Pair of Mirror Segments Aligned and Bonded in Module	3.6 (two reflection)	Based on optical metrology or full illumination X-ray measurement; The alignment process contributes 1.2 arcsecs to the two-reflection HPD
Mirror Module as Built and Tested on the Ground	3.8 (two reflection)	Based on full illumination X-ray measurement; Module structure distortion due to gravity, thermal distortion, and inter-mirror-shell alignment etc. combine to contribute 1.2 arcsecs to the two-reflection HPD
Flight Mirror Assembly as Built and Tested on the Ground	4.0 (two reflection)	Based on partial X-ray tests and on optical alignment data and modeling and analysis; The co-alignment of modules contributes 1.2 arcsecs to the FMA's final HPD

3 Mirror Segment Fabrication

Mirror fabrication starts with *forming mandrels and flat glass sheets* and ends in mirror segments fully measured and documented to meet three sets of requirements:

1. Optical figure requirements: 2.3 arcsecs HPD (one reflection) in its “free-standing” form (see Table 4);
2. Effective area requirements: must be coated with ~15 nm of iridium to enhance its X-ray reflectivity;
3. Mechanical integrity and dimension requirement: properly cut to size for installation into module housing and smooth, fracture-free edges to prevent breakage under launch loads.

Each mirror segment is completely characterized by the following quantities (see Section 6.1 for detailed descriptions):

1. **Average radius:** a single number measuring the average cylindrical radius of curvature
2. **Radius variation,** also known as roundness error: an array of numbers describing the radius deviation as a function of azimuth
3. **Average cone angle:** a single number expressed in degrees
4. **Cone angle variation,** also known as **Delta-Delta-R** error: an array of numbers describing the cone angle deviation as a function of azimuth
5. **Average sag:** a single number describing the axial second order
6. **Sag variation:** an array of numbers describing the sag deviation as a function of azimuth
7. **Residual or Remainder:** typically a two-dimensional array of numbers; Sometimes loosely described as axial figure errors to emphasize the nearly one-dimensional nature of x-ray optics.

When describing axial figure errors, for the sake of clarity and convenience, we typically use three spatial regimes: (1) low frequency figure that covers the spatial periods from 200mm to ~20mm; (2) middle frequency figure that covers the spatial periods from ~20mm to ~2mm; and (3) high frequency figure that covers the spatial periods from ~2mm to about ~2 μ m. The high frequency figure is also referred to as the micro-roughness.

Mirror fabrication consists of five steps: (1) forming mandrel preparation, (2) thermal slumping, (3) cutting to size, (4) coating, and (5) metrology. These steps, their development status, and issues that need to be addressed, are described in Sections 3.1 through 3.5.

3.1 Forming Mandrels

Technology and expertise exist in many industrial companies and government institutions that can adequately meet IXO flight mandrel quality and production schedule requirements. There is no need to develop mandrel fabrication technology. The purpose

here is to obtain adequate numbers of forming mandrels to enable this technology development program under stringent budgetary and schedule constraints. We use existing facilities and personnel at Goddard Space Flight Center and Marshall Space Flight Center (see Figure 2) to re-work three existing pairs of mandrels, which were previously figured and polished to ~ 7 arcsecs HPD (two reflections). For historic reasons these mandrels have a focal length of 8.4m.

This part of the effort is to bring these three pairs of mandrels to meet the requirement of 2.2 arcsecs HPD (two reflections) or 1.5 arcsecs HPD (one reflection). This effort started in October 2008. As of April 2009, the first pair (F489P and F489S) had been figured to 1.5 arcsecs HPD (one reflection) and 1.9 arcsecs HPD (one reflection), respectively. Table 2 shows the schedule for the forming mandrel fabrication effort. While the F489S mandrel does not precisely meet the 1.5 arcsecs HPD requirement, it is close enough for the purpose of developing the slumping process. It may be re-worked when the other two pairs are completed.

Table 5. Start and completion dates for the fabrication of the three pairs of mandrels. The first pairs (F489P and F489S) has been completed and delivered.

Mandrel Pair	Fabrication Start Date	Fabrication Completion Date	Figure Quality
F489P and F489S	October 2008	April 2009 (Delivered)	1.5 and 1.9 arcsecs HPD, respectively (one reflection)
F494P and F494S	May 2009	September 2009	NA
F485P and F485S	October 2009	March 2010	NA

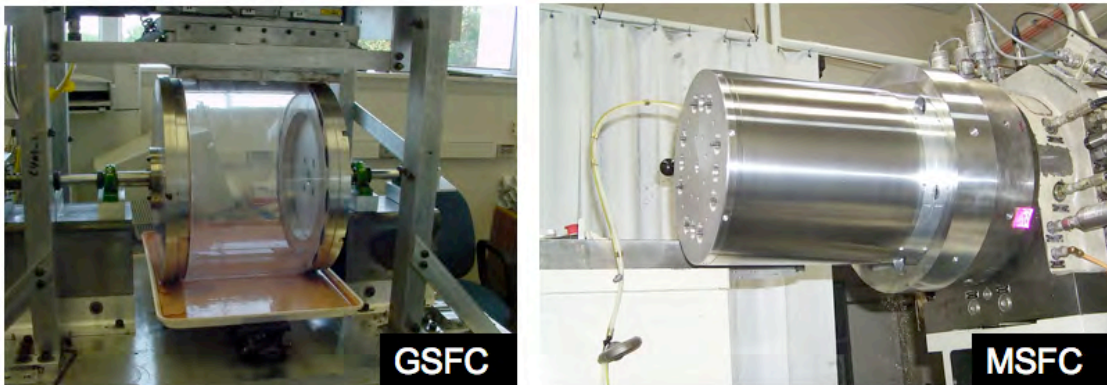


Figure 2. In-house forming mandrel fabrication at GSFC (left) and MSFC (right). The GSFC works uses the traditional polisher whereas the MSFC work adopts a precision machining technique plus an innovative electro-mechanical finishing technique.

We are also pursuing a potentially low cost, rapid fabrication approach to mandrel manufacturing at the Marshall Space Flight Center. These stainless steel mandrels are being fabricated via precision turning, and then polished using electro-mechanical polishing techniques. Areas of investigation include permanent deformation during the thermal cycling of repeated slumping cycles, release layer approaches, mandrel accuracy, and size limitations, see Figure 2.

Each mandrel will be fully characterized before its delivery to the mirror fabrication development laboratory at Goddard Space Flight Center. The metrology data will be used for comparing mandrel and substrate figures.

3.2 Slumping

The slumping process creates a high-fidelity glass substrate that is a replica of the forming mandrel. The process is illustrated in Figure 3. For the sake of clarity we make a distinction between mirror substrate and mirror segment. A mirror substrate is a bare piece of glass that has been slumped and cut to size but *not yet coated* with a sufficient thickness of iridium to enhance its X-ray reflectivity. A mirror segment is a substrate that has been coated with ~15nm of iridium. Table 4 summarizes the requirements and the status of mirror substrate fabrication.



Figure 3. A graphic illustration of the glass slumping process (left panel). A flat sheet of glass is placed atop a precision figured forming mandrel. As the temperature ramps up from room temperature to near the glass sheet's transition temperature, the glass sheet deforms and sags under its own weight to conform itself to the mandrel, replicating its figure. The right panel shows two mandrels with substrates on them that have come out of the oven.

Table 7 is a summary of the substrate fabrication status. Each parameter of the typical substrate is juxtaposed with its requirement. Current mirror substrates do not meet requirements primarily because of two reasons. The first reason is inadequate forming mandrels used, which has been addressed in Section 3.1. We have been using forming mandrels that have an HPD of 7 arcsecs (2 reflections), which were fabricated to meet a previous mission requirement of 15 arcsec HPD. Recent effort in upgrading forming mandrel quality has produced the first mandrel pair F489P and F489S. Both mandrels are already being prepared for slumping. First results are expected for July 2009. By the end of the first quarter of 2010, we expect to be using three pairs of mandrels, all of which meet the 1.5 arcsec HPD (one reflection) figure requirement.

Table 6. Summary of the status of glass slumping. The work reported in this table has been done using forming mandrels that have a figure quality of 7 arcsecs HPD.

Mirror Substrate Quantity	Unit	Reqmnt	Typical Substrate	Comment
Average Radius Error	μm	<20	<20	Believed to meet requirement, further metrology and confirmation to be conducted (See Section 3.4)
Radius Variation	μm (RMS)	<0.5	0.10	Met requirement
Average Cone Angle Error	Arcsec	<0.5	Accurate measurement in progress	Believed to meet requirement, further metrology and confirmation to be conducted (See Section 3.4)
Cone Angle Variation	Arcsec (RMS)	<0.5	0.4	Met requirement
Average Sag Error	μm	<0.1	~0.25	Sources of uncertainty: (1) mandrel sag measurement, (2) mirror metrology mount, and (3) null lens calibration (See Section 3.5)
Sag Variation	μm (RMS)	<0.1	0.3	Sources of error: (1) iridium coating stress, (2) mirror metrology mount distortion, and (3) null lens calibration (See Section 3.5)
Low Frequency Axial Figure Error (Spatial period: 200-20mm)	μm (RMS)	<0.10	0.15	Forming mandrel figure dominant source of error (See Section 3.1)
Middle Frequency Axial Figure Error (Spatial period: 20-2mm)	μm (RMS)	<0.01	0.03	Mandrel release layer dominant source of error (See Section 3.1)
High Frequency Axial Figure Error (Spatial period: 2mm to $1\mu\text{m}$) (aka μ roughness)	Angstrom (RMS)	<10	8	Met requirement

The second reason that the current mirror substrates do not meet requirements is excessive mid-frequency errors that are caused by a sprayed-on boron nitride coating on the forming mandrels. The BN coating, serving as a release layer, is necessary to prevent the glass sheet from permanently adhering to the mandrel surface at high temperatures.

While the sprayed-on boron nitride (BN) release layer enables the very accurate replication of the low-order figures, it has middle spatial frequency errors (wavelength ~ 2 to ~ 20 mm), which currently dominate the figure errors of the resulting substrate. The way to reduce or eliminate these mid-frequency errors is creating a release layer that is as smooth as possible in the mid-frequency band. We are pursuing two independent methods to address these errors.

3.2.1 Boron Nitride Release Layer

The first method is to continue improving the application of the existing BN release layer. Better application of BN layer includes finer and better spraying methods and sputtering of boron nitride.

The mid-frequency errors of the spray-on boron nitride layer are not caused by the size of the boron nitride hexagonal crystals themselves. These crystallites (or platelets) are typically $0.02\mu\text{m}$ thick and $0.3\mu\text{m}$ in the other two dimensions, too small to cause the mid-frequency errors with spatial periods of 2 to 20 mm. It is the agglomerates of these boron nitride crystallites that are formed during the spray process that cause the coating thickness to vary, resulting in the mid-frequency errors. We will add at least one industrial homogenizer in the spray process to minimize agglomeration of small boron nitride crystallites. Using one or more industrial homogenizer will enable the continuous agitation of the boron nitride slurry, therefore preventing any significant agglomerates from forming. We will continue to improve the buffing process to remove any residual agglomerates.

We have also been working with sputter applications of boron nitride coatings as a release layer. In one approach, reactive deposition, B is DC magnetron sputtered in an N_2 atmosphere of a few milli-torr. At the surface of the mandrel, the B reacts with the N_2 to produce BN. Biasing the mandrel to a temperature of $\sim 200^\circ\text{C}$ promotes the formation of hexagonal boron nitride (hBN). We have already applied such coatings, albeit with only limited success. X-ray diffraction has confirmed the formation of hBN. The coatings are hard, durable, and specular in finish, matching well the underlying mandrel surface. So, if they were to work as a release layer, such coatings would address the mid-frequency problem. Our problems to date center around both eliminating O_2 from the coating, and ensuring that every boron atom is bonded to a nitrogen atom. At present, achieved B:N ratio is about 1.2, far higher than the desired ratio of unity. Both of these problems enable oxygen bonds to cross-link the two surfaces, mandrel and substrate, resulting in sticking. And in fact, our first attempts have not resulted in successful release.

We are proceeding with a number of incremental improvements to our coating facility that will reduce the oxygen content and decrease the B:N ratio. We will install a cryo pump on the deposition chamber, effectively pumping water vapor (the source of most oxygen), and we will experiment with deposition rates and nitrogen partial pressures, as well as the location of nitrogen gas feed, to decrease the B:N ratio. Then we will retest the release characteristics of the layer. After getting good release, we will fine tune parameters to improve figure characteristics of the slumped substrate. A potential cause for concern is that we are uncertain what benefits are provided, if any, by the platelet-like nature of the sprayed BN, which will be absent in the sputtered coating. If low friction between the two surfaces is critical, and the result of BN platelets sliding against one another, the reactively sputtered hBN may release, but yield poor figure replication.

A second means of sputtering BN is possible. Using a BN target, a BN vapor stream can be produced via RF magnetron sputtering. We will attempt to use this BN coating as a release layer if reactively deposited BN does not work. Drawbacks of RF sputtered BN are that (a) the deposition rate is much lower than reactive DC sputtering, and (b) the deposited coating will be amorphous BN, which may not provide the low friction characteristics of hBN.

3.2.2 Platinum and Platinum-Gold Alloys Release Layer

Platinum and platinum-gold alloys have been used successfully as release layers for hot and molten glass. Both can be either sputtered or evaporatively deposited on glass, while maintaining the optical characteristics (figure, mid-frequency, and micro-roughness) of the underlying glass substrate. We are investigating the use of these two materials as thermal forming release layers. In this approach, 40nm of Pt or Pt/Au (in an 85:15 to 90:10 ratio) are sputtered directly onto the pre-slumped mirror substrate, as opposed to the previous cases where the release layer is on the forming mandrel. The coated substrate is placed directly on the fused silica forming mandrel and slumped. This approach has already been shown to provide a clean release between the substrate and the mandrel (both by us and by colleagues at Osservatorio Astronomico di Brera in Italy). If the substrate conforms closely enough to the mandrel, then the substrate mid-frequencies should match the mandrel mid-frequencies, which can be made optically smooth. This would eliminate the mid-frequency errors. What must be demonstrated is whether this works as well as sprayed BN with respect to low-frequency mirror figure.

We believe this approach works by preventing contact between the mostly SiO₂ mirror substrate and an oxidized surface of the SiO₂ mandrel. At high temperatures, we think the weak oxygen bonds can be broken and crosslink between the two surfaces (substrate and mandrel). Using a non-oxidizing material (the Pt or Pt-Au) as a barrier allows for release. In addition, the thermal forming results in good adhesion between the slumped mirror substrate and the release layer coating. Coating the mirror before slumping allows the annealing process to take place in the presence of mirror coating stresses.

Table 7 shows the timelines of these investigations.

Table 7. Summary of mandrel release layer studies and schedule.

Boron Nitride Release Layer	February 2009 – September 2010	(1) Spray-on boron nitride: better and finer agitation; (2) Reactive coating of boron nitride using magnetron; (3) RF-sputtering of boron nitride
Alternative Release Layer	October 2009 – Decembe 2010	(1) Use of pure Pt as a release layer; (2) Use of Pt and Pt-Au alloys as a release layer

3.3 Post-Slumping Cutting

After slumping, each substrate is cut to the size required for alignment and bonding into a module housing. Currently we use a template that has been designed and precisely fabricated for each mandrel size. The template references the mandrel's edge to enable accurate marking of the substrate while it is still on the forming mandrel. This process ensures the proper orientation of the substrate's optical axis with respect to the substrate's edges.

A hot-wire glass cutting technique was invented to cut the substrate along the marks made using the template, as shown in Figure 4. This process has proven to produce the required dimensionally precise (~50 µm) and fracture-free edges. Figure 5 shows a comparison of glass edges resulting from three glass cutting techniques: (1) a laser cutter, (2) a diamond (or carbide) tip; and (3) the hot-wire cutter. The hot-wire technique results in facture-free edges meeting IXO requirements. No further development is necessary.



Figure 4. Post-slumping cutting of the substrate using a hot-wire. The glass cracks under thermal stress. The crack trails Nichrom hot-wire which is heated with an electric current. There is no material loss. It leaves a very smooth and fracture-free edge as shown in Figure 5.

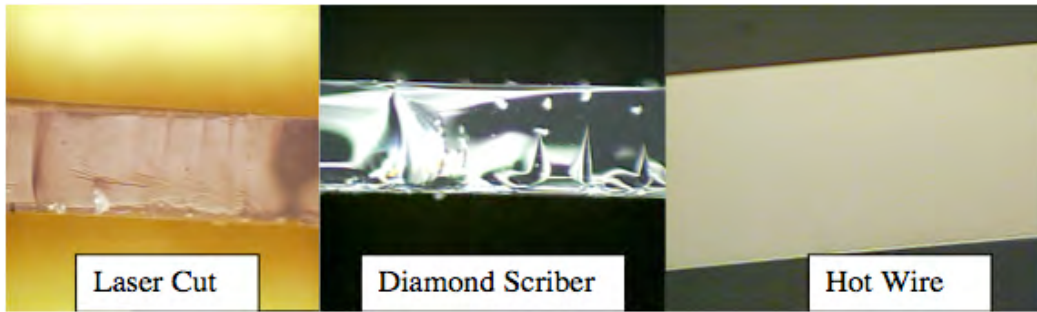


Figure 5. A comparison of glass edges resulting from the three different cutting techniques.

3.4 Coating

Bare glass surfaces need to be coated with ~ 15 nm of iridium to enhance their X-ray reflectivity, thereby increasing their effective area. In general, sputter coating has a higher density than evaporative coating, which translates into a higher X-ray reflectivity. We have successfully sputtered glass substrates with an iridium coating that meets microroughness requirements using equipment shown in Figure 6. The issue to be addressed is the reduction of coating stress that distorts the mirror figure.



Figure 6. Coating chamber that can accommodate 4 magnetrons simultaneously: two for coating concave surfaces and two for coating convex surfaces. **Left panel:** the exterior of the chamber; **Right panel:** the turntable inside the chamber. The chamber is approximately 60 cm in diameter and 25 cm in height.

Figure 7 shows the results of an experiment demonstrating that iridium coating stresses the thin mirror segment, producing azimuthally varying sag error. In this experiment, a series of four coatings are sputtered. After each coating the mirror segment is measured for its sag variation as a function of azimuth. In general the sag variation has the shape of

the letter “M”. As more and more iridium is sputtered on the mirror segment, while the general shape of the “M” remains more or less the same, the amplitude increases proportionally.

We will investigate two methods to reduce or eliminate the effect of the coating stress. The first method is to reduce or eliminate *the stress itself*. We will increase the argon pressure used during the coating process, which in general is expected to decrease the stress by a factor of 5 to 10 from ~5 GPa to 0.5 GPa (see, e.g., Windt, D., 1999, J. Vac. Sci. Technol. B, Vol. 17, p. 1385). Finite element analysis has shown that 0.6 GPa stress causes less distortion than requirement and is therefore acceptable.

The second method is to reduce the effect of the iridium coating stress by balancing it with another stress with an opposite sign: using a bi-layer coating of chromium and iridium. Under our specific coating conditions, chromium film has tensile stress whereas iridium film has compressive stress. When combined in the appropriate thicknesses, a chromium and iridium bi-layer coating could have near-zero net stress on the mirror substrate. Recent experimental work by Dr. David Windt of Reflective X-ray Optics, LLC provides conclusive evidence demonstrating the feasibility of this approach, see Figure 8.

In both of these cases we first investigate the coating parameters and conditions using small wafers which enable easy and quick measurement of net stress. Once coating conditions and parameters are understood and determined, we will implement the coating for mirror segments. This work is being done in two phases as described in Table 8.

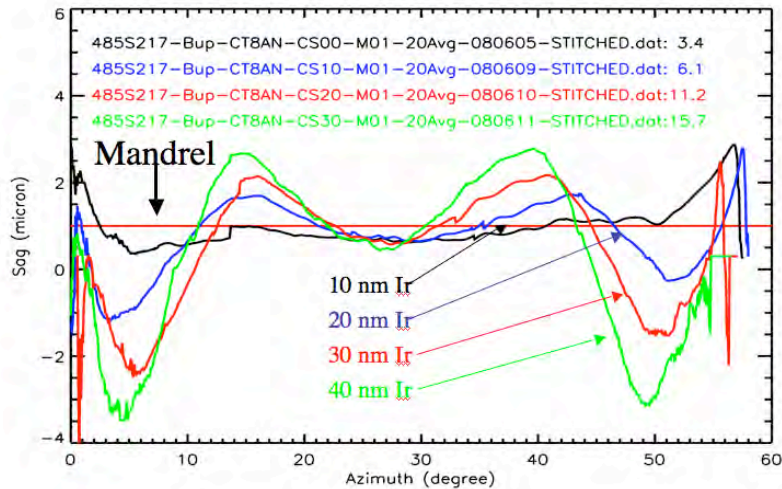


Figure 7. Empirical data showing conclusively that Ir coating can change the mirror sag as a function of azimuth. The different "M-shaped" curves are from the same mirror coated with different amounts of Ir. The amplitude of “M” shape is proportional to the Ir thickness.

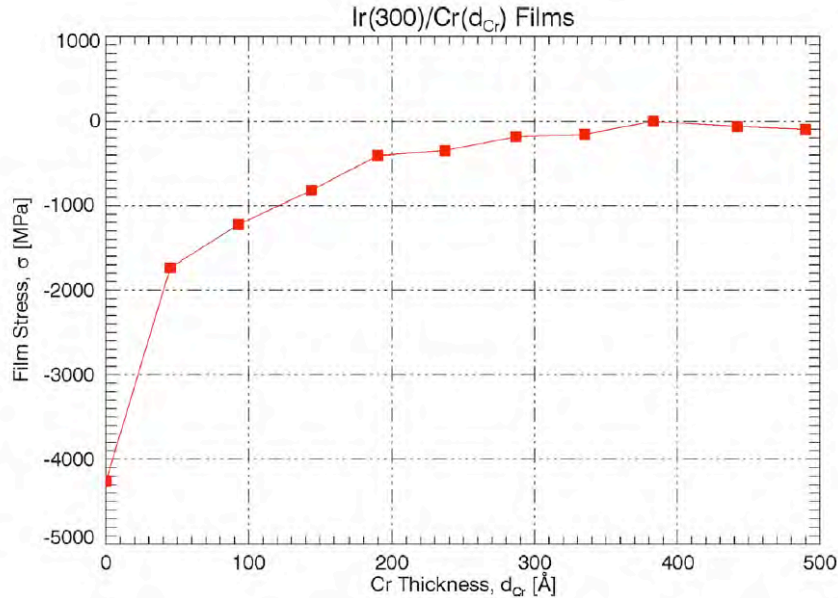


Figure 8. Net stress of an iridium/chromium bi-layer coating as a function of the chromium layer thickness. (Courtesy David Windt, Reflective X-ray Optics, LLC, New York, New York)

Table 8. Two phases of coating study and their timelines.

Phase-I: Investigation of coating conditions and parameters using small wafers	January 2009 – March 2010	(1) Systematic study of coating stress (using standard silicon and/or glass wafers) as a function of Ar gas pressure and film thickness for both iridium and chromium coatings; (2) Determination of optimum coating parameters to achieve minimum or near-zero coating stress; (3) Experiment with Cr+Ir bi-layer coating to achieve near-zero stress coating
Phase-II: Implementation for coating mirror segments	April 2010 – September 2010	Systematic coating of mirror substrates; Detailed comparison of figures before and after coating; Detailed comparison between finite element analysis results and coating results

3.5 Metrology

The objective of mirror segment or substrate metrology is to fully and completely measure all the parameters (as described in the beginning of Section 3) of each mirror segment accurately and with acceptable speed (to accommodate the eventual mass production schedule). Metrology provides necessary feedback to the mirror fabrication process, as well as providing a “free-standing” figure baseline for the mirror segment, against which the subsequent steps of mounting, alignment, and bonding can be measured.

As of May 2009 we have procured and commissioned all necessary equipment to completely and definitively measure each mirror segment: (1) a 10-inch aperture high speed interferometer, (2) two cylindrical null lenses and associated rotational and translational stages, (3) a cylindrical coordinate measuring machine, (4) a vertical long trace profilometer (VLTP), and (4) a Zygo Newview 5000 profilometer for microroughness measurement.

Table 5 shows the mirror parameters and the corresponding instruments that can measure them. Each parameter is measured by at least two totally independent instruments to ensure a quantitative understanding of any potential systematic errors.

When a mirror segment is properly supported, all of its parameters can be easily measured with the existing equipment. The crucial area of work is in understanding the mirror segment support while it is being measured. Currently we have two ways of supporting a mirror segment: (1) Cantor-tree mount (see **Figure 9**) and (2) Suspension mount (see **Figure 11**). We will systematically model each of these two methods and conduct experiments to quantitatively compare the measurement results from the two independent and rather dissimilar methods. We will also conduct finite element analysis to quantitatively account for any systematic difference, which is most likely caused by gravity.

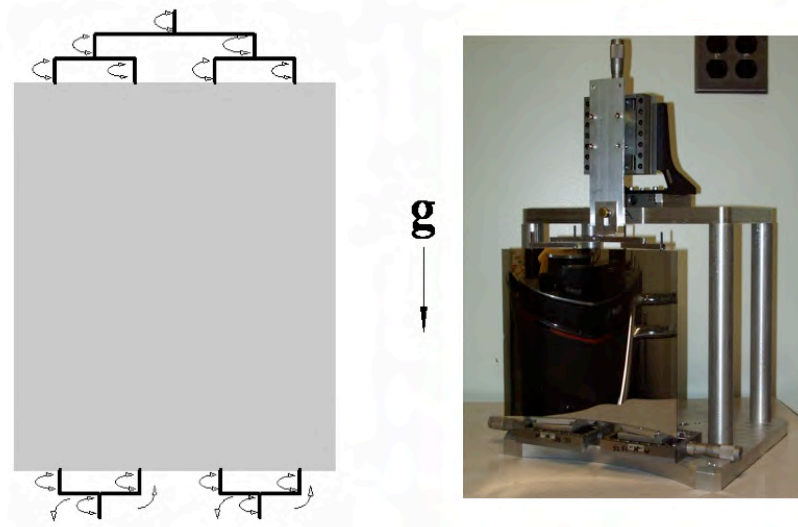


Figure 9. The Cantor-tree mount of a mirror segment. Left panel is an illustration of the 8 points contacting the mirror segment. The right panel is a photograph of a real implementation. In this mount the mirror segment is in the most vertical direction possible, resulting in the least amount of distortion by gravity. The bearings near the contact points minimize distortions from other forces.

Our strategy is to first achieve repeatability and then understand and reduce systematic uncertainties. Systematic uncertainties include wave front error of the null lens, distortion of mirror segment by gravity and other repeatable forces.

Figure 10 shows a mapping between the graphs from a complete measurement and the mathematical parameters of a mirror segment. Currently because of an electronic readout limitation, we have not yet been able to measure the average radius and the average cone angle. This problem will be addressed by the end of 2009.

Table 6 details the specific tasks and timelines of their starts and completions.

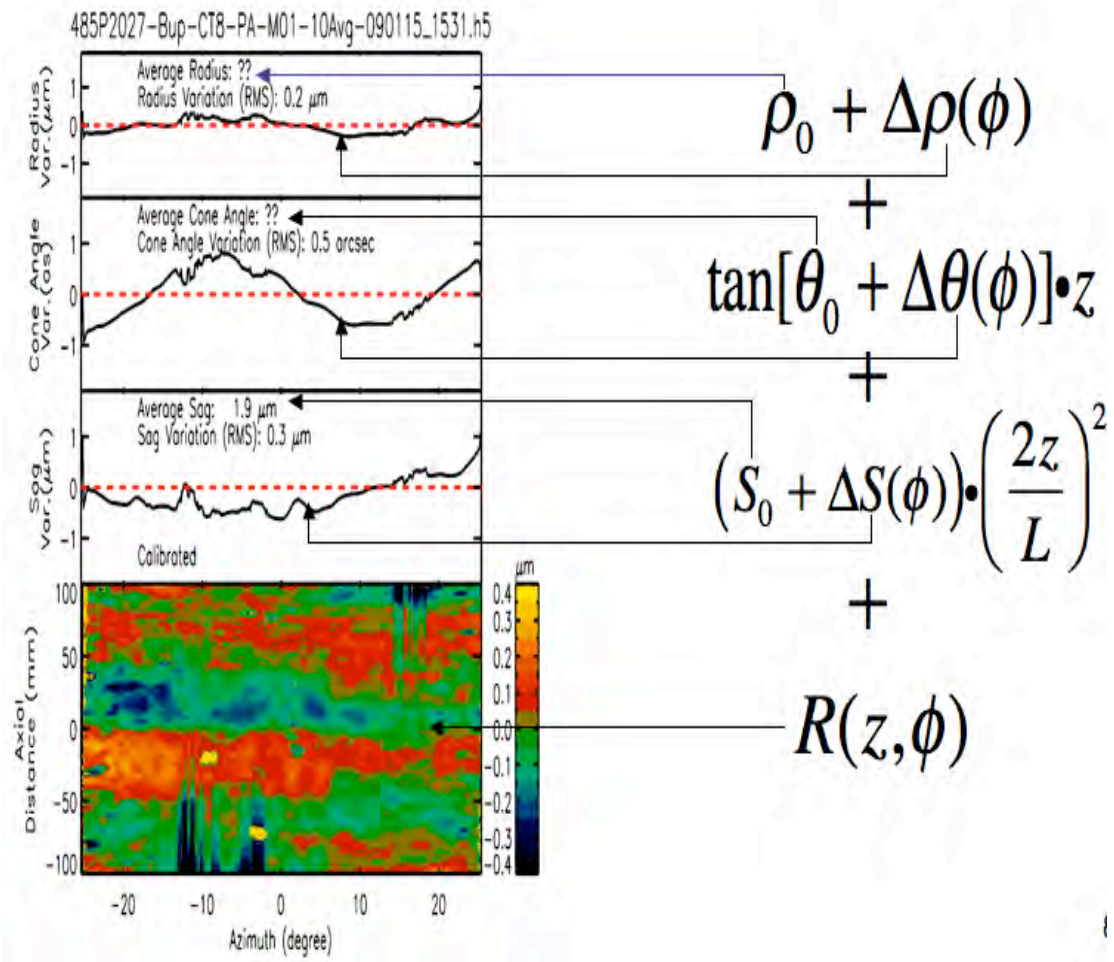


Figure 10. Mapping of the mathematical terms of a mirror segment and their measurements. The average radius and average cone angle, marked with “??” are not yet measured. (see Table 10.)

Table 9. Correspondence between mirror segment parameters and their measurement instruments. All of the relevant parameters except microroughness are measured with more than instrument to ensure consistency and understanding of systematic effects.

Mirror Parameter	Interferometer and Null Lens	Coordinate Measuring Machine (CMM)	Vertical Long Trace Profilometer (VLTP)	Zygo Newview 5000 Profilometer
Average Radius	Yes (after proper stage readout is implemented)	Yes		
Radius Variation	Yes	Yes		
Average Cone Angle	Yes (after proper stage readout is implemented)	Yes		
Cone Angle Variation	Yes	Yes		
Average Sag	Yes	Yes	Yes	
Sag Variation	Yes	Yes	Yes	
Low Frequency Figure	Yes	Yes	Yes	
Middle Frequency Figure	Yes		Yes	Yes (after stitching mechanism is implemented)
High Frequency Figure (μ Roughness)				Yes

Table 10. Two phases of mirror segment metrology technique development and their detail timelines and implementations.

Phase-I: Repeatability	May 2009 - December 2009	Measurement of average radius and average cone angle	(1) Implement electronic readout of tip-tilt stages to measure mirror segment's average cone angle; (2) Implement a micrometer to measure the distance between the null lens focus and the mirror segment surface to determine the average radius.
		Null Lens Stability	Perform experimental verification that placement of the null lenses does not introduce random or systematic distortions to their wave fronts
		Mirror Mounts	Systematic investigation of placement of mirror segments on (1) Cantor-tree mount and (2) Suspension mount; Design and implementation of new Cantor-tree mounts and suspension mounts.
Phase-II: Accuracy	January 2010 – December 2010	Study and understanding of measurement systematic errors	(1) Fabrication and commission of a metrology standard that is certified by the National Institute of Standards and Technology; (2) Calibration of null lens wave front errors; (3) Detailed comparison of measurement results using different mounts; (4) Detailed finite element analysis to understand systematic errors of mirror mounts.

4 Mounting, Alignment, and Bonding

After a mirror segment has been fully measured and characterized and otherwise qualified, it is to be mounted, aligned, and bonded into a mirror module housing structure. This process of mounting, aligning, and bonding must meet two distinct requirements:

1. It must preserve or maintain the optical figure of the mirror segment, and
2. It must provide enough support and stability such that the mirror segment can withstand the launch loads without degrading its optical or mechanical integrity.

We are pursuing in parallel two independent developments based on different philosophies: a passive, or traditional, method and an active method. The passive method

seeks to preserve the figure of the mirror segment throughout the bonding process, while the active method seeks to improve the mirror segment figure using actuators prior to bonding.

In December 2010, when both the passive and active approaches have reached TRL-5, we will conduct a comprehensive technical review of the two developments and take stock of the lessons learned and techniques developed from both approaches and select the method that is better in all four aspects of mounting, alignment, and bonding: (1) accuracy, (2) speed, (3) cost, and (4) compatibility with requirements at higher system levels.

4.1 Passive Approach

The passive method follows the traditional opto-mechanical practice of minimizing stresses external to the mirror segment, which distorts optical figure. These stresses can be minimized by carefully limiting the forces which interface with the mirror. Good opto-mechanical designs seek to hold the mirror in its “free state” using kinematic mounts which constrain a mirror in six degrees of freedom. The passive approach uses the precision figure of the mirror segment as the guide throughout the mounting, alignment, and bonding process. We will meet the figure requirement by examining the steps involved in bonding a mirror and minimizing the error contribution of each step using standard engineering practices.

The passive method is a three-step process for each mirror segment:

1. *Mounting*: The first step is to mount and bond the mirror segment **temporarily** onto a **strongback**, as shown in Figure 11, converting the flexible mirror segment into a *de facto* rigid body that can be handled, characterized, transported, and aligned. Small screws with rounded tips are threaded through a strongback. The screw tips are wetted with epoxy and the strongback is slowly adjusted into position with optical stages so that the tips of the screws contact the mirror surface at the same time. Once the epoxy has cured, the strings supporting the mirror are cut and removed, and the mirror is now held by the small (1-2mm diameter) epoxy bonds to the strongback.
2. *Aligning*: The mirror segment is located and aligned properly in position and orientation using precision stages under the monitoring of an optical beam with grazing incidence Hartmann tests. This step is simple and easy since the mirror segment is effectively a rigid body.
3. *Bonding*: Once alignment is achieved, the mirror segment is bonded at several locations permanently to the module housing structure. The transfer process from temporary bonds to permanent bonds is shown in Figure 12. The requirement on this process is to permanently bond the mirror segment at several points without introducing stress or displacement so that, when the temporary bonds are removed, the mirror segment does not suffer either any displacement which degrades alignment, or any distortion which degrades figure error.

4. *Removing the transfer mount:* After the permanent bonds have cured, the temporary bonds to the transfer mount are released and the transfer mount is removed.

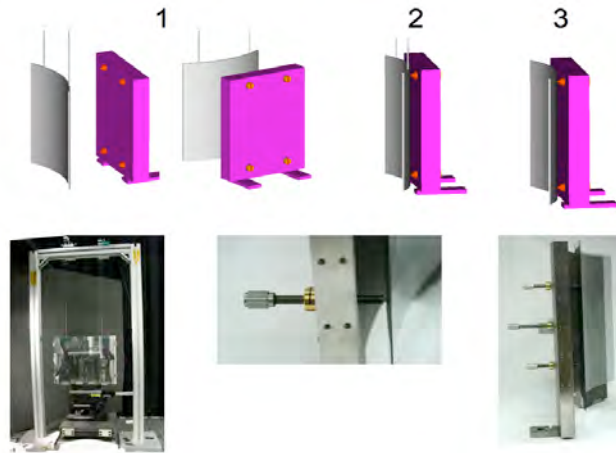


Figure 11. An illustration of the process of converting a flexible mirror segment into a de-facto rigid body. The upper CAD drawings show clarity. The lower photos show the implementation. (1) suspended mirror with strongback; (2) strongback bonding pin interface with mirror; (3) strongback holding a mirror via bonded pins. Once a mirror segment is bonded to the strongback, shown in the lower-right picture, it can easily transported, aligned, and otherwise manipulated using any number of standard optical techniques.

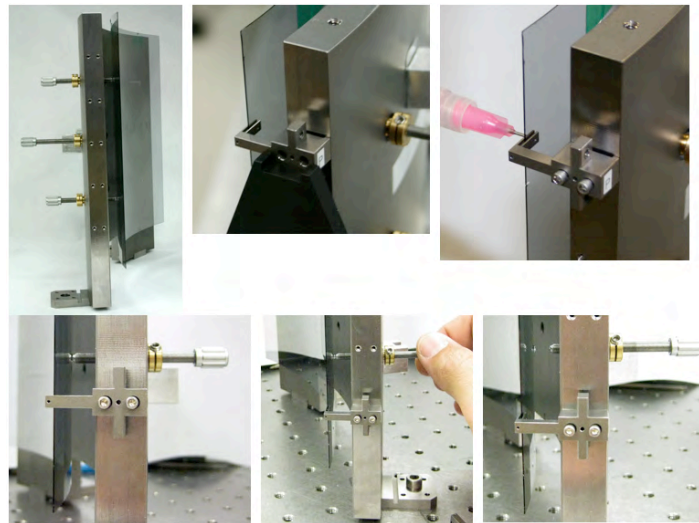


Figure 12. Experiment proving the concept of transferring a mirror segment from temporary bonds to permanent bonds on the same strongback to develop the process of transfer. Left to right starting from top: (1) mirror segment on its temporary mount, (2) bonding tab is attached; (3) epoxy injected to bond mirror and tab; (4) epoxy cures; (5) temporary bond being removed; and (6) temporary bond screw retracted and the mirror segment has been successfully transferred.

A key parameter in both temporary bonding and permanent bonding is the number of bonds. In general, fewer bonds mean less distortion. As such the preservation of the optical figure calls for the mirror segment to have *as few bonds as possible*. On the other hand, withstanding the launch loads calls for *as many bonds as possible*. Extensive load analysis has led to the conclusion that 8 bonds are needed to enable the mirror segment to withstand launch loads. Our strategy is to begin the development effort with 4 bonds and, as we learn and understand the various factors of the bonding process, we will grow the number of bonds from 4 to 8 and minimize distortion every step of the way.

We have successfully bonded mirror segments repeatably both temporarily and permanently with 4 bonds and conducted a number of X-ray tests, one of which is shown in Figure 13. Table 11 shows the parameters of a typical mirror segment at different stages of the bonding process. These numbers show that a 4-point bonded mirror segment can meet requirements. In the next year we will systematically study every aspect of bonding and further reduce these errors and increase the number of bonds from 4 to 8.

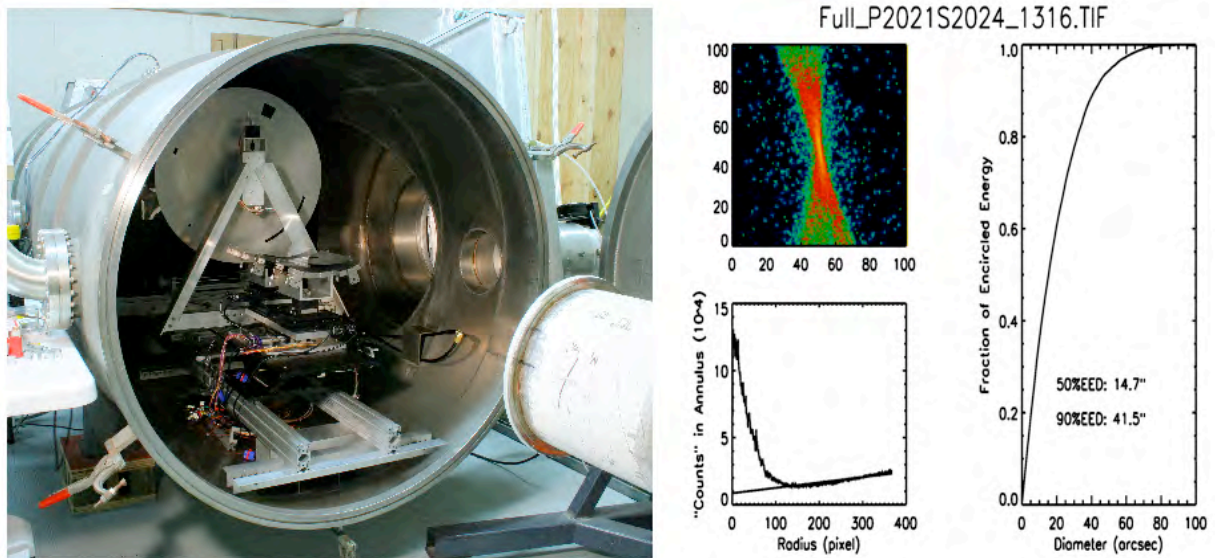


Figure 13. A pair of mirror segments bonded and aligned in a vacuum chamber ready for a full illumination X-ray test (**left panel**); X-ray test results (**right panel**). In the right panel, the upper left picture shows the X-ray image obtained using Ti K X-rays (4.5 keV); the lower left graph shows the X-ray count in an annulus as a function of the radius of the annulus, the straight line representing the expected background; the graph on the right shows the encircled energy fraction as a function of the diameter, indicating an HPD of 14.7 arcsecs.

Table 11. Figure parameters of a mirror segment, labelled as 489P2021, at different stages of bonding and X-ray testing. The number of bonding points in the process is 4.

Mirror Segment 489P2021						
	Radius Variation (RMS μm)	Cone Angle Variation (RMS arcsec)	Average Sag (μm)	Sag Variation (RMS μm)	Low Frequency Figure (RMS μm)	Mid-Frequency Figure (RMS (μm))
"Free Standing"	0.39	0.22	0.73	0.30	0.12	0.04
Temporary Mount	0.07	0.83	0.10	0.42	0.14	0.04
Permanent Mount (before X-ray Test)	0.13	0.89	0.57	0.48	0.14	0.04
Permanent Mount (after X-ray Test)	0.16	0.51	0.39	0.34	0.20	0.03

We are conducting an intense study of the error sources for temporary and permanent bonding. The primary sources of error for the temporary bonding experiment are:

1. epoxy shrinkage
2. thermal expansion
3. gravity sag
4. procedural and design issues

Epoxy shrinkage during curing causes the mirror to move and also induces small stresses into the mirror. It is reduced by selecting epoxies with very low shrinkage such as Hysol 9313 and a UV-cure epoxy such as Optocast 3415. Shrinkage, when highly repeatable on the sub-micron level, can be designed around. The key is to design all the bond interfaces with uniform epoxy volume and geometry so that when the epoxy shrinks, the glass moves as a rigid body in the expected manner and for an expected distance. Experiments in this area are ongoing, and sub-micron repeatability has been achieved in a small-scale glass-to-metal bonding fixture.

Thermal expansion issues are reduced by (1) temperature control in the laboratory, and (2) selection of materials which closely match the CTE of D263 glass which is 6.2 ppm/C. Some strongbacks of D263 have been made and used, but they are difficult to machine to tight tolerances. The most easily workable metal is an alloy of Titanium with 15% Molybdenum (Ti-15Mo) which has a CTE in the range of 6.4 – 7.1 ppm/C depending on the vendor and the precise specification requested. We are using material cut from a custom mill run block of Ti-15Mo with a CTE of 6.434 ppm/C. Another thermal expansion issue is the thermal lag, or thermal inertia, of components within the

temporary bond assembly. The D263 glass is thin with a large surface area and it tracks the room temperature changes more rapidly than the larger Titanium strongback. Thermal lag is reduced by lightweighting the strongbacks as much as possible and maintaining tighter dynamic limits in the room air conditioning system.

The effects of gravity sag are easily understood with finite element analysis. Several aspects of the strongback design have been analyzed to reduce the effects of gravity sag. Strongback thickness, pin diameter, pin location, and strongback orientation relative to gravity are just some of the design parameters analyzed to date.

Procedural and design issues are the ones that are often discovered during hands-on testing in the lab. A typical issue is how to position the strongback so that the pins contact the mirror simultaneously. This was solved by using a precision linear stage, and pre-aligning the mirror prior to wetting the pins. Another issue is dispensing the same volume of epoxy with the same viscosity on each pin to avoid differential shrinkage causing mirror distortions. This is improved with the use of an automated dispensing machine commonly found in medical applications. Study in these areas is ongoing.

Another key design issue for temporary bonding is optimizing the number and location of the bond points. Finite element analysis has determined that the optimal locations for the pins for the mirrors currently used in our lab experiments are at 133 mm azimuthal and 200mm axial. Analysis is ongoing in tandem with hardware development.

The development of the passive approach proceeds in four phases. In each of these phases, the natural progression is to start with bonding a mirror segment at four locations and progress to eight locations. In Phase-I, we bond single mirror segments on temporary mounts, concentrating on the minimization of figure distortion. In Phase-II, we conduct experiments to transfer mirror segments from temporary mounts to permanent mounts, concentrating on minimizing the loss of figure quality in the transfer process. In phase III, we bond single mirror segments and align and transfer them to a housing simulator, as shown in Figure 14, first a primary and then a secondary, minimizing both figure distortion and alignment error. In phase-IV, we will achieve co-alignment among multiple pairs of mirrors, reaching TRL-5.

Table 12 shows the timelines of this development.

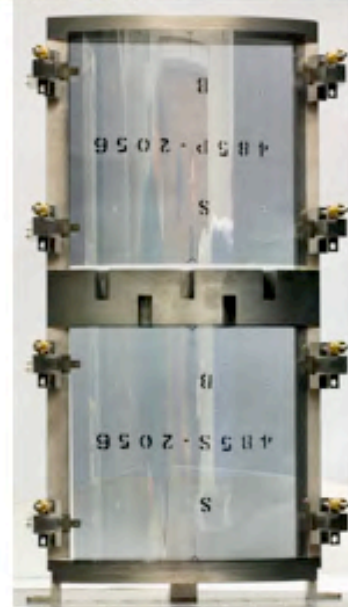
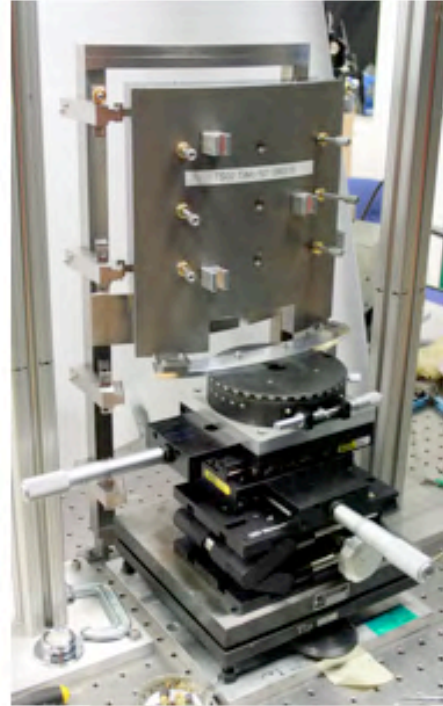


Figure 14. Mirror housing simulator is populated with a mirror pair using the strongback and a four sliding tab assemblies per mirror. Clockwise from upper-left: (1) the titanium structure to which mirror segments are aligned and bonded; (2) mirror segment on its temporary mount being aligned with a set of precision stages; (3) both primary and secondary mirror segments bonded to the structure; (4) an amplified picture of the bond.

Table 12. Four phases of development of the passive mounting, alignment and bonding approach. In each phase, the progress is from 4 bonding points per mirror segment to 8 which will enable the mirror segment to withstand launch loads.

Phase-I: Temporary Mount of Mirror Segments	April 2008 – December 2009, 2009	(1) Temporarily bond mirror segments at <i>four</i> points to a strongback; (2) Temporarily bond mirror segments at <i>four</i> points to a strongback (3) Conduct X-ray tests to achieve good X-ray images
Phase-II: Permanent Mount of Single Mirror Segments	October 2008 – December 2009	(1) Transfer mirror segments from temporary bonds to permanent bonds: 4 bonds; (2) Transfer mirror segments from temporary bonds to permanent bonds: 8 bonds; (3) Conduct X-ray tests to achieve good X-ray images
Phase-III: Alignment and Bonding of Single Mirror Pairs	May 2009 – February 2010	(1) Align and bond single pairs of mirror segments into a housing simulator, initially at four points, then at eight points; (2) Conduct optical metrology and X-ray tests Completion of TRL-4 Demonstration
Phase-IV: Alignment and Bonding of Multiple Mirror Pairs	August 2009 – November 2010	(1) Co-align and bond multiple pairs of mirror segments into a housing simulator, initially four bonding points per mirror segment and then eight bonding points per mirror segment; (2) Conduct X-ray tests and environment tests Completion of TRL-5 Demonstration

4.2 Active Approach

The active approach takes advantage of the flexibility of the mirror segments to adjust the average cone angle and cone angle variation. In this approach, radial displacements produced by actuators at the mirror segments' forward and aft ends are used to correct the mirror segments' tilt errors (pitch and yaw) and adjust cone angle to minimize the alignment aberrations of focus error and coma. After achieving the best possible focus, the mirror segment is permanently bonded to the module housing structure. After the permanent bonds have cured, the actuators are disengaged and removed.

The active approach supports each mirror segment at 10 locations, five equally spaced at each of the forward and aft ends. All the actuators drive in the radial direction. By driving all the actuators at one end of the mirror radially in or out by an amount $dx(\theta) = \delta/\cos(\theta)$, where δ is a constant, θ is the azimuthal position of the actuator (mirror midline is at $\theta = 0$ deg), and $dx(\theta)$ is the desired actuator motion in the radial direction, the mirror can be made to tilt in or out from the optical axis, or pitch. Varying the actuator motion linearly from one side of the mirror to the other ($+\theta_{\max}$ to $-\theta_{\max}$), in addition to the 1/

$\cos(\theta)$ scaling, or $dx(\theta) = \delta \cdot (\theta/\theta_{\max}) / \cos(\theta)$, the mirror is made to twist, which optically is equivalent to a tilt about its surface normal, or yaw. Finally, by varying the $dx(\theta)$ quadratically with θ , i.e., $dx(\theta) = \delta \cdot [3(\theta/\theta_{\max})^2 - 1] / \cos(\theta)$, the cylindrical radius at one end of the mirror segment can be changed, effectively changing the cone angle.

Using this ability to warp and tilt a mirror segment, along with a Hartmann test as *in-situ* alignment metrology, we can adjust a mirror segment to minimize aberrations at the nominal focal plane prior to bonding the mirror in place. It is important to note that while there is no real adjustment freedom for mirror decenter or average radius error, these errors produce coma and focus error, which can be corrected with much smaller mirror motions via tilts and cone angle changes, respectively. Thus, we have the capability to correct mirror alignment errors due both to the installation of the mirror in the housing, as well as due to potential focal length errors.

The active approach consists of four steps for each mirror segment: mounting, adjusting, bonding, and removing actuators.

Mirror bonding clips (Figure 15) are separately epoxied to each end of the mirrors at the appropriate locations. (This can be done off-line on a separate bonding fixture). The primary mirror is positioned in its housing at approximately the correct distance from the system optical axis using a coordinate measuring machine (CMM) with a few micrometer accuracy. Nano actuators are affixed to the aft end of the primary (see Figure 16) and are adjusted to minimize radial runout of the primary aft end. Once that is accomplished, the bonding clips are epoxied to the rails. After the epoxy is cured, the adjusters are decoupled from the bonding clips and removed. Once the aft end of the primary mirror is bonded, adjusters are attached to the bonding clips at the forward end and are coarse adjusted using the CMM.

At this point, alignment proceeds using the Hartmann test. Alignment of the primary is geared to three purposes: (1) aligning the segment optical axis to the system optical axis by minimizing off-axis coma, (2) adjusting the segment focal length to the correct value and centering the segment to the optical axis (via the CMM), and (3) minimizing the cone angle variation error at the focal plane by adjusting the actuators. This last operation serves two purposes. First, it removes any cone angle variation imparted by using the CMM to locate the aft attachment points of the mirror. Second, it allows us to correct low frequency (≈ 2 cycles/segment width) cone angle variation, improving upon segment figure.

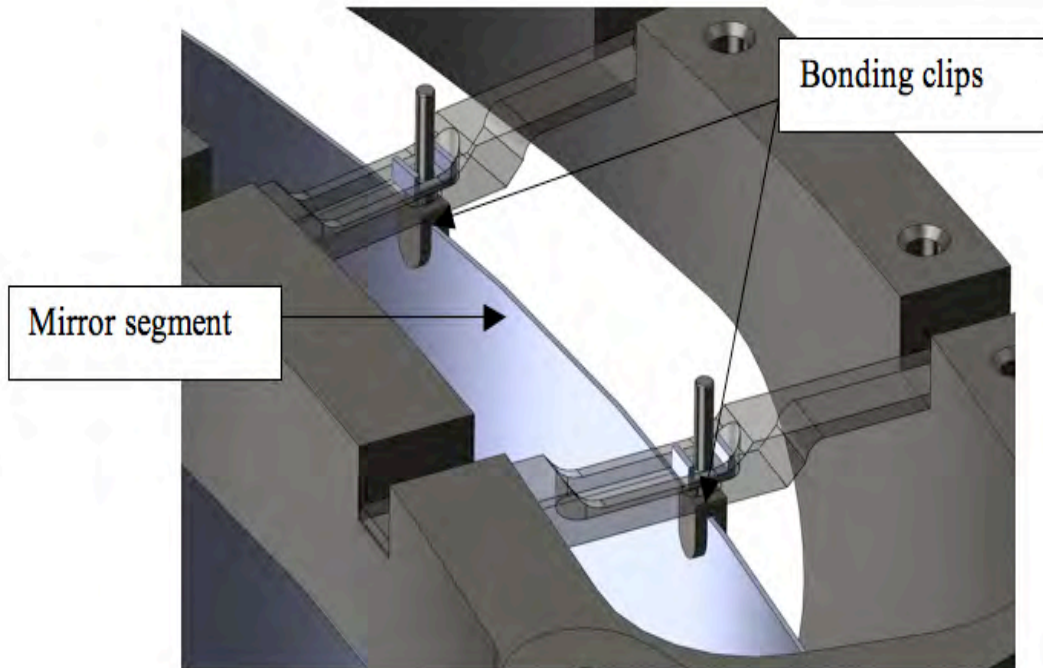


Figure 15. CAD drawing of mirror bonding clips, shown in the OAP. The bonding clips are the ‘U’ shaped pieces with the long vertical posts.

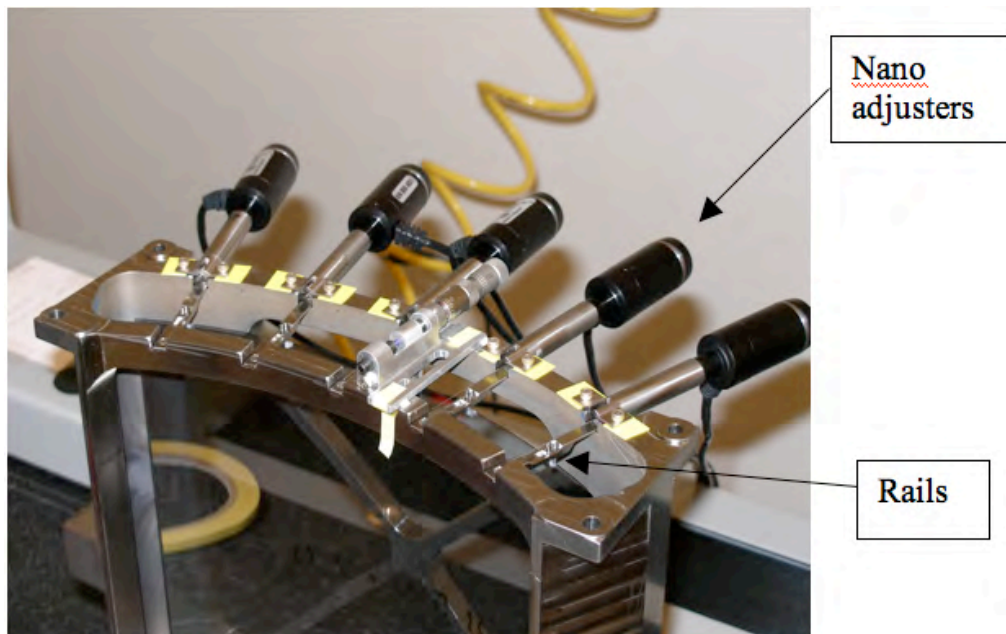


Figure 16. A view of the nano-adjusters and the housing rails. Note the wires coming from the nano-adjusters; the adjusters are computer controlled, a feature that lends itself to a feedback-controlled closed-loop alignment system. Note that a mirror is installed in this housing.

In order to align multiple shells of mirrors, the next alignment step would be to repeat the process with the next radially inboard primary mirror. This allows the primaries to be made confocal. Then, the process is repeated for the outermost secondary mirror, wherein the CMM alignment and bonding process is used for the forward end of the secondary. Now, when aligning the aft end of the secondary using the adjusters and Hartmann test, we adjust the secondary mirror tilts to minimize coma resulting from misalignment of the secondary to the primary (a much more sensitive source of error than off-axis coma for the primary). Focus is adjusted for the secondary to get the mirror pair to focus at the correct system focus. And again, lastly, we can adjust the actuators individually to attempt to minimize cone angle variation. The secondary is then bonded, the adjusters removed, and one moves on to the next inner primary segment. In this way the alignment order is P1 (outermost primary), P2 (second outermost primary), S1, P3, S2, ..., always allowing us to make the primary mirror confocal prior to aligning the secondary segment. We also note that this approach allows the reflective surface of the mirror under alignment to be exposed to normal incidence optical metrology. This enables us to measure the final mirror figure of the as-bonded, aligned mirror segment. Lastly, the entire alignment operation is performed with the optical axis vertical, as can be seen in Figure 17. This minimizes the self-weight-distortions due to gravity.

We have successfully aligned and bonded a single pair of mirror segments (see Figure 17). The alignment precision is consistent with budget requirements. Figure measurements are being made, and it is necessary to demonstrate that any figure degradation is at acceptable levels or less. Repeating the process is required. During the alignment process we have demonstrated that:

1. Focus can be corrected deterministically by adjusting secondary mirror cone angle in a convergent process of Hartmann metrology, compute focus error, compute required adjuster motions, adjust, and remeasure;
2. Adjuster motions as described earlier herein can be used to correct for coma introduced by secondary to primary misalignments, including both pitch and yaw, similarly in a deterministic and convergent process;
3. Alignment does not change as a result of bonding and the removal of the actuators;
4. Mirror response to adjuster motions is repeatable to within measurement accuracy (sub-arcsec), and predictable such that the adjustment process converges in 2 to 3 iterations at most;
5. Segment pair cone angle variation error (delta-delta-radius error) can be corrected using the adjusters - $\sim 1/3$ the effective azimuthal figure error was corrected as part of the alignment;
6. Alignment metrology met system level allocated errors; and

7. Mirror alignment met system level allocated errors.

Enhancements to the active alignment hardware will be necessary for the alignment and mounting of multiple shells, and X-ray and environmental testing. These include modification of bonding rails to allow mounting of more than one mirror pair, and development and fabrication (as required) of interface hardware for X-ray and environmental testing. Developmental activities will include: replacing the large actuators with much smaller ones; proper cable dressing, to minimize actuator loading of the structure; improved thermal control of the alignment; incorporation of in-situ (to the vertical test tower) figure metrology, and the procedural development activities necessitated by aligning multiple shells for the first time. We also will develop the closed-loop feedback control system, wherein data acquired by the Hartmann test is used to calculate adjuster motions, and those motions are then commanded by the central computer. Once the motions are complete, a new Hartmann scan will be automatically initiated and the results updated.

Similar to the development of the passive method, the active method development is carried out in three phases. In the first phase, we will achieve repeatability in bonding single mirror segments, improving or at least preserving their optical figure and achieving good focus. In the second phase, we will actuate and bond single mirror pairs to demonstrate that we can align and bond two mirrors simultaneously to achieve both good figure and focus, doing so with repeatability.

In the third phase, we will install multiple pairs (at least two) of mirrors into a housing that are substantially similar to a flight housing but it is not lightweighted to save money and time. It will serve to demonstrate that not only multiple pairs can be co-aligned by adjusting the focus of individual mirrors, but also that the small amount of stress imparted on the mirror segments do not affect their neighbors alignment.

Table 8 shows the three phases of the development.

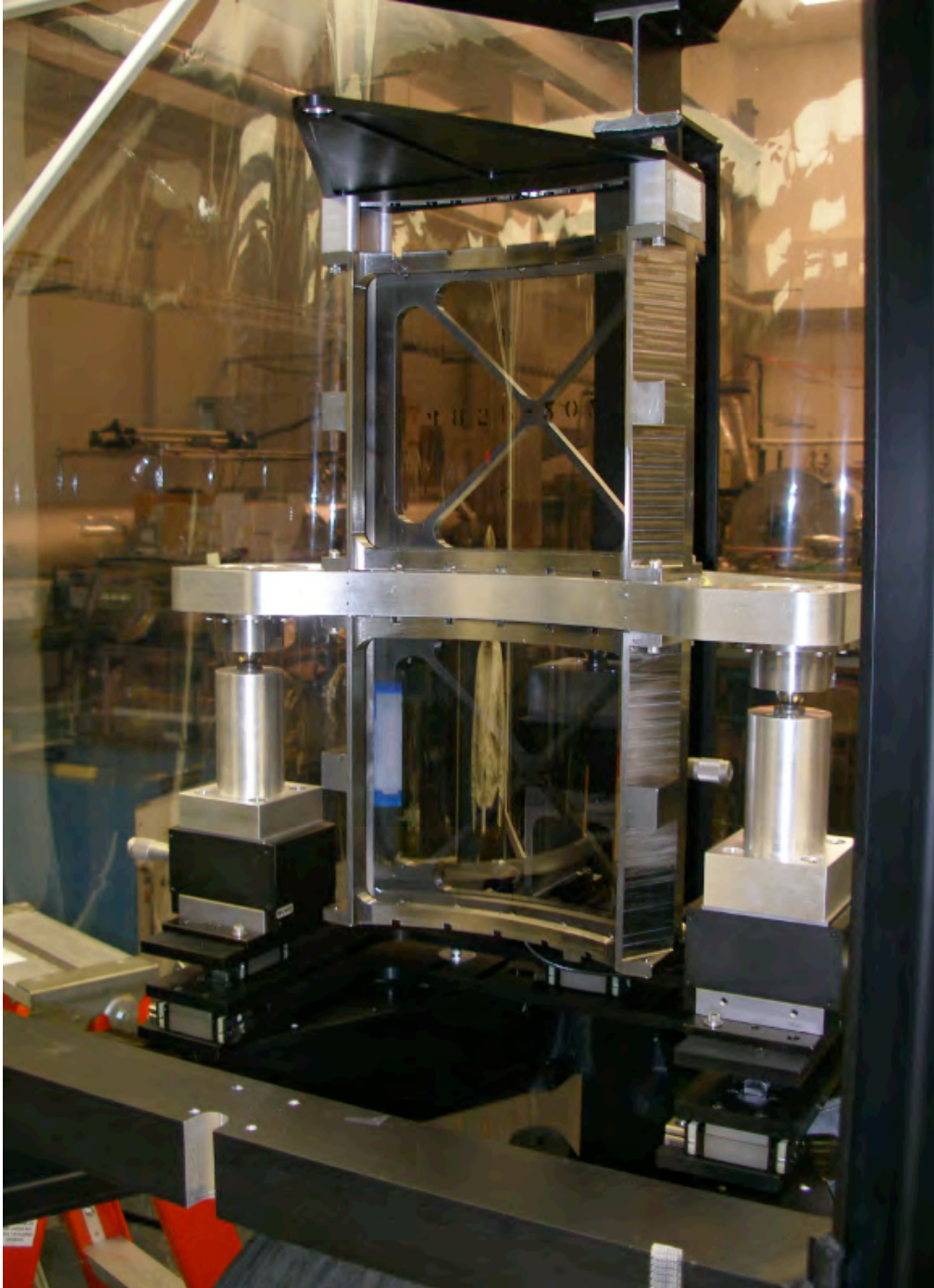


Figure 17. Picture of an aligned, bonded primary and secondary mirror pair in the housing sitting in the vertical test tower. The gravity vector is ‘down’ in the picture. Telescope forward is ‘up’ in the picture. The test beam for the Hartmann test is folding into the aft end of the telescope with a 45 deg fold flat just visible at the bottom of the picture. A large retro-flat is located above the primary. The Hartmann test as employed here is a ‘double-pass’ test, resulting in twice the error sensitivity.

Table 13. Three phases of development of the active alignment approach.

<p>Phase-I: Bonding of Single Mirror Segments</p>	<p>October 2007 – August 2009</p>	<p>(1) Actuate and bond individual mirror segments; (2) Demonstrate correction and achieved pre-determined change of cone angle and or average radius; (3) Demonstrate that the process is repeatable</p>
<p>Phase-II: Bonding and Aligning of Individual Pairs</p>	<p>October 2008 – November 2009</p>	<p>(1) Bond and align pairs of primary and secondary mirror segments; (2) Conduct optical metrology and X-ray tests to obtain X-ray images for comparison with predictions based on optical metrology</p>
<p>Phase-II: Bonding and Aligning of Multiple Pairs</p>	<p>December 1, 2009 – July 1, 2010</p>	<p>(1) Bond and co-align multiple pairs of mirror segments in a simulator module housing; (2) Conduct optical metrology and X-ray tests to obtain images for comparison with predictions based on optical metrology; (3) Conduct environment tests; Completion of this phase leads to Phase-III in Section 5.</p>

5 Mirror Module Design and Construction

This technology development will culminate in the design and construction of at least one mirror module that meets all requirements. Parallel to the development activities described in Sections 3 and 4, formal engineering study and design are underway to synthesize knowledge and experience gained and implement them in designing the FMA and the modules. This effort begins with a preliminary design phase and goes through Development Testing, Selection of Alignment Approach (Passive or Active), Detailed Design and Analysis, and finishes in the Fabrication of a flight-like module that undergoes a complete battery of flight qualification tests.

5.1 Preliminary Design

Starting with the IXO mission angular resolution, effective area, mass, and schedule requirements as well as preliminary structural requirements, including natural frequency and quasi-static design loads, we have developed a preliminary design, as shown in Figure 1. Much of the design work applies to both the passive and active approaches. The preliminary design was developed in parallel with the FMA and IXO observatory designs to ensure compatibility with the overall mission concept. Trade and sensitivity

studies relating to module structure topology, material selection, and thermal control were performed to arrive at a preliminary module design. Structural, thermal, and opto-mechanical analyses were performed to demonstrate the design is capable of meeting requirements, as shown in Figure 18. Integration and test accommodations are also considered in the preliminary design. At the completion of the preliminary design phase the concept was reviewed and the basic trade study results, CAD models, and FEA results were validated.

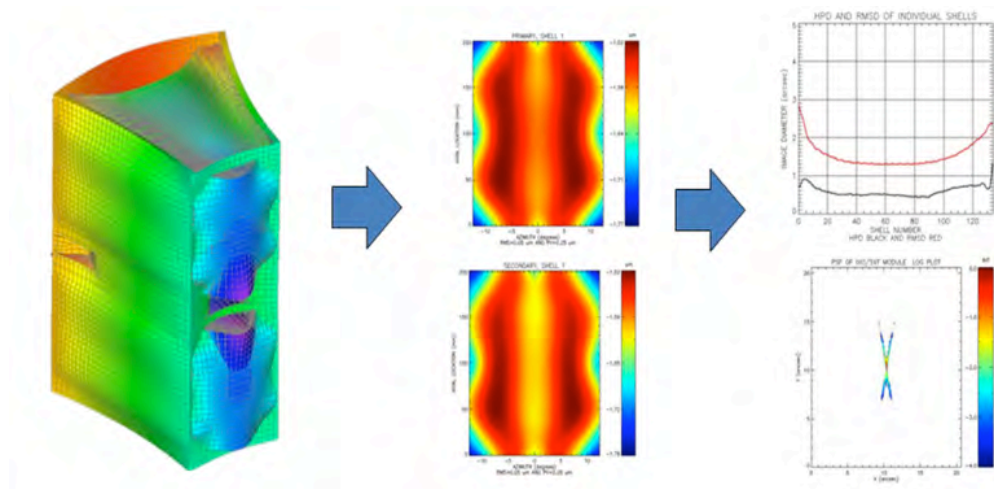


Figure 18. Structural and thermal loads are applied to a detailed finite element analysis, mirror segment figure distortions are output to ray tracing software, and performance is predicted for each segment and entire module.

5.2 Development Testing

Development testing and mirror structural analysis were performed to ensure that the behavior and strength of the glass segments in the flight environments are well understood. The response to loading environments was investigated via static load testing, modal testing, sine and random vibration testing, and acoustic testing including a successful acoustic test of three closely spaced segments at EELV qualification levels (Figure 19). Mirror segment response including modes and stresses correlated well with analysis predictions. Pre- and post-test mirror figure measurement show the mirror figure does not change as a result of loading environments. A shock test simulating actuation of the pyrotechnic spacecraft separation devices is currently being developed.

Sufficient strength of the glass segments is ensured by performing a simple proof test on each segment before it is bonded into a module. Per NASA-STD-5001, the segments are subjected to the ultimate stress allowable used in design with a proof test factor of 1.2. The ultimate stress allowable used for design and proof testing is determined by the acceptable segment scrap rate and the strength distribution of the slumped glass. The strength of the slumped segment is a function of the distribution of surface cracks, and is typically described by the two parameter Weibull distribution. For example, using a 1 in

1000 scrap rate, the ultimate strength of our slumped mirror segments is 40.0 MPa based on the Weibull parameters determined through extensive materials testing.

The quasi-static loads used to determine the maximum glass stress for a segment mounted into a module are based on the launch vehicle requirements and the dynamic response of the FMA and spacecraft. The SXT analysis team has performed sine loads analysis using detailed Finite Element Models (FEMs) of the preliminary FMA and spacecraft designs. Quasi-static loads in X, Y, and Z were enveloped to provide appropriately conservative loads for this phase of the project.

Positive stress margins have been determined for the mirror segments by using these loads and the 40 MPa stress allowable on the glass. The margins of safety were calculated in accordance with the principles required by NASA-STD-5001 and GSFC-STD-7000 (GEVS), which require a Model Uncertainty Factor (MUF) and a 3.0 factor of safety for glass. The glass strength allowable of 40 MPa was determined by selecting the scrap rate of 1 in 1000. In summary, materials testing of slumped glass, extensive analysis with appropriate factors of safety, and verification with development testing of mounted segments, ensures that the segments can be launched successfully.

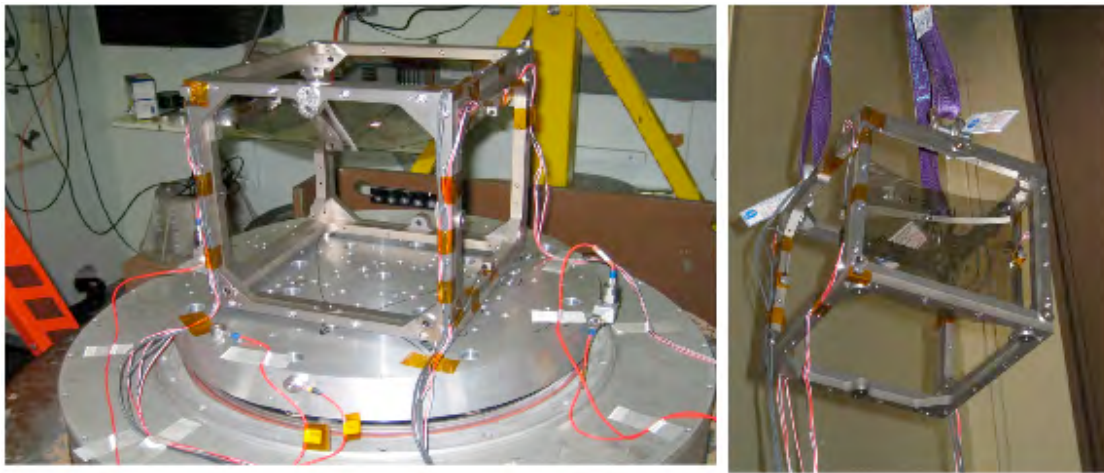


Figure 19. Left panel: Vibration test of a mirror segment bonded in a structure simulating a module housing; Right panel: Acoustic test of the same mirror.

5.3 Selection of Alignment Approach

Based on the alignment and bonding technology development and preliminary module designs, the design which is most compatible with requirements will be chosen. Possible discriminators include demonstrated angular resolution, mass, effective area, assembly speed, mechanical robustness, and compatibility with system level requirements.

5.4 Detailed design and analysis

A detailed module design using the selected alignment and mounting approach will be developed to demonstrate TRL 6. Standard design and analysis methods will be employed to ensure the design meets requirements including detailed structural, thermal, and opto-mechanical analysis (Figure 20). Results of the development tests will be leveraged in this effort to ensure the performance will be bounded by the analysis predictions. Flight-light design loads will be developed by sine response analysis of the coupled spacecraft/FMA/module FEMs with an appropriate Model Uncertainty Factor (MUF). The TRL 6 demonstration module will be based on the preliminary FMA module design, but modified to accommodate the segments produced by the available mandrels. The three mandrels available will be used to produce flight quality segments for the module and the remainder of the module will be filled with segments with representative mass and stiffness.

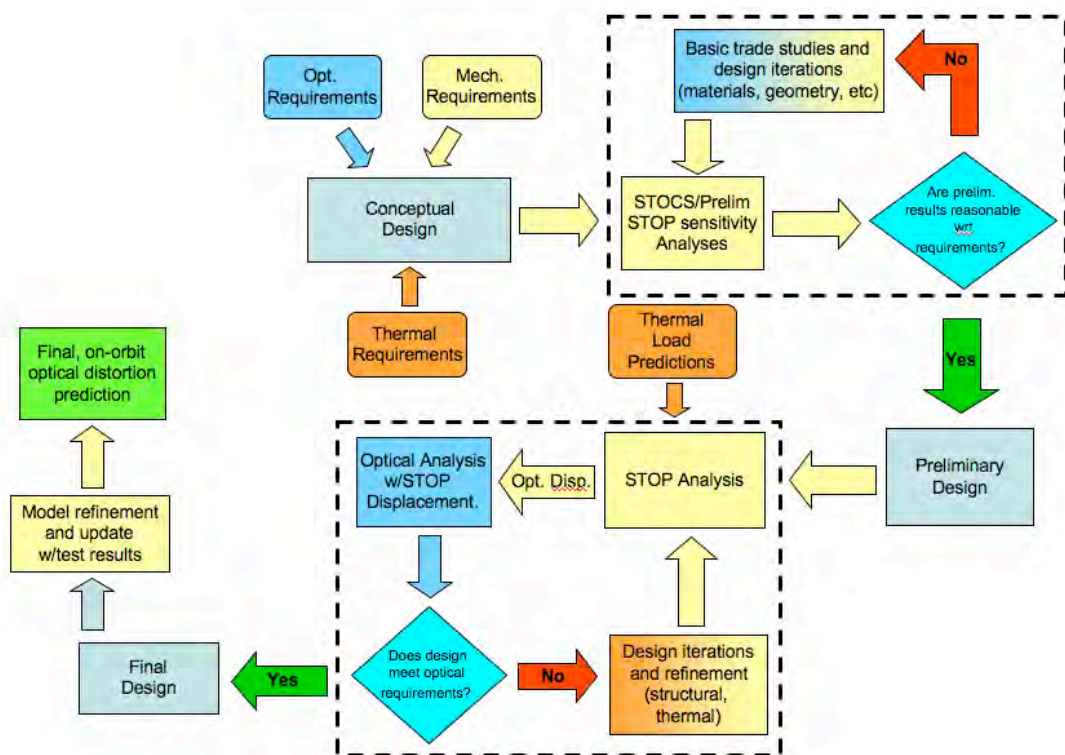


Figure 20. Structural, thermal, and optical performance (STOP) analysis flow chart. This analysis cycle will be used at the system (FMA), subsystem (module), and component (mirror segment) levels for maximum confidence in results.

5.5 Fabrication and Testing

The TRL 6 demonstration module will be fabricated, assembled, and populated with segments as described above. This process will demonstrate the end-to-end module fabrication process including alignment and bonding into a flight-like structure. A typical optomechanical test sequence will then be completed including X-ray testing,

random vibration testing, acoustic testing, and thermal/vacuum testing (Figure 21). Full illumination X-ray testing verifying angular resolution and effective area at the required energies will be performed before and after each structural/thermal test.

The six phases of the mirror module (mechanical and thermal) design and construction are shown in Table 14.

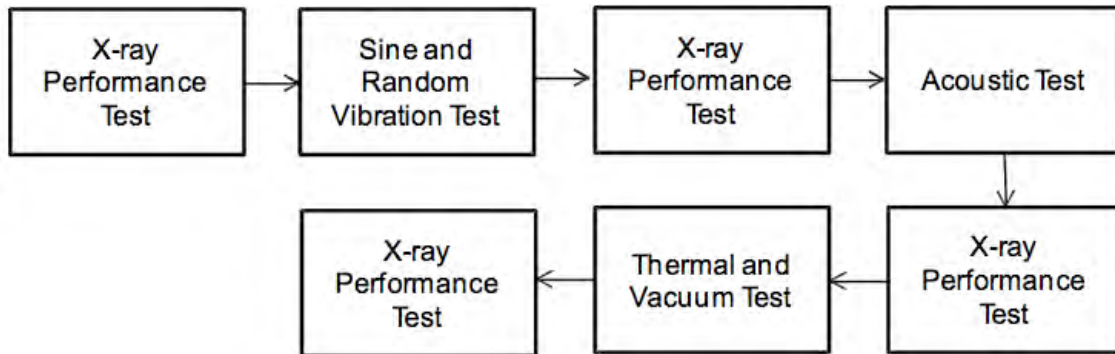


Figure 21. Flow of a battery of tests to qualify the mirror module for TRL-6.

5.6 Large Segment Alignment and Bonding Demonstration Testing

The mirror segments and module that have been built up and tested so far represent the smallest mirror shells of the IXO flight mirror assembly. We believe that it is prudent and necessary to perform analysis and conduct experimental verification to address the various scaling issues as we move to larger mirror segments and mirror modules. We will procure forming mandrels that are close to the largest radius of curvature, approximately 3.2m in diameter and verify each of the manufacture and integration steps. Once larger mandrels are available, the selected alignment and bonding technology will be demonstrated with the largest segments in the FMA design. Mechanical analysis of the module design can be reliably extended to segments with larger radii and azimuthal span. We will conduct necessary experimental verification of the analysis results, including building and testing a module with the largest mirror segments.

Table 14. The six phases of work to design and construct a flight-like mirror module that meets all requirements.

Phase-I: Preliminary Design	July 2008 – June 2010	(1) Derivation of requirements from observatory top level requirements: angular resolution, effective area, etc. (2) Mode and load analysis; (3) Compatibility analysis; (4) Preliminary design and FMA and modules
Phase-II: Development Testing	August 2008 – October 2009	(1) Measurement of glass CTE; (2) Measurement of glass breaking strengths; (3) Measurement epoxy properties; (4) Vibration and acoustic test of individually bonded mirror segments; (5) Conduct necessary tests to verify analysis results
Phase-III: Selection of alignment and bonding approach (Passive or Active)	December 2010	(1) Define selection criteria; (2) Conduct review of all technical details of the two approaches
Phase-IV: Detailed design and Analysis	December 2010 – March 2011	(1) Detailed structural, thermal, and opto-mechanical analysis; (2) Flight design load analysis; (3) Investigation of model uncertainty factor; (4) Accommodation of available mandrels; (5) Conduct an independent review of design and analysis
Phase-V: Fabrication and Test	January 2011 – June 2011	(1) Construction of flight-like module; (2) X-ray test to measure PSF and effective areas at several X-ray energies; (3) Conduct vibro-acoustic tests to Atlas-V qualification levels; (4) Conduct thermal vacuum tests; (5) Conduct one more round of X-ray measurement to verify PSF and effective areas; and (6) Conduct environmental test until and module fails to establish conservative structural integrity criteria.
Phase-VI: Demonstration of aligning and mounting of largest mirror segments	January 2011 – December 2011	Perform opto-mechanical, thermal analysis of the largest possible mirror segments and its behavior under the same conditions as the module that has been built and tested.

6 Appendix

6.1 Mirror Segment Description

IXO mirror assembly adopts the traditional Wolter-I design. Each mirror shell consists of a parabolic primary and a hyperbolic secondary. In a polar coordinate system (ρ, ϕ, z) with its origin at the focal point of the parabolic and hyperbolic system, the primary and secondary mirrors can be described as

$$\rho_p^2 = (d + z_0 + z)^2 - (z_0 + z)^2,$$

$$\rho_h^2 = (d + z)^2 e_h^2 - z^2,$$

where three parameters, d, z_0 , and e_h , uniquely specify the mirror shell properties. In practice, two conditions are imposed to optimize the design:

1. the parabolic shell and the hyperbolic shell must have the same radius at the focal length ($z = f$), specified to be ρ_0 ; and
2. to maximize the effective area, the grazing angles at this intersection must be the same for both the primary and secondary.

Therefore a focal length (f) and a shell radius at the P-H intersection (ρ_0) completely and uniquely determine the geometry of a shell. The three parameters (d, z_0 , and e_h) are determined can be computed using the following equations

$$\begin{aligned} d &= \rho_0 \tan \theta, \\ z_0 &= \frac{\rho_0}{2} \left(1 + \frac{1}{\tan \theta} - \tan \theta \right), \\ e_h &= \sqrt{\frac{\rho_0 \tan 3\theta + f}{\rho_0 \tan \theta + f}}, \end{aligned}$$

where $\theta = \frac{1}{4} \tan^{-1} \frac{\rho_0}{f}$ is the grazing angle at the P-H intersection plane.

In day-to-day work, it is more convenient and useful to Taylor-expand the parabolic (or hyperbolic) description at the mid-point of its axial extent. As it turns out, for both parabolic and hyperbolic mirrors, an expansion to only the second order would be more than adequate for the purpose of IXO mirrors:

$$\rho(z) = \rho_0 + c_1 z + c_2 z^2,$$

where ρ_0, c_1 , and c_2 are constants that uniquely prescribe each mirror shell. As far as mathematical prescriptions go, all these constants are azimuth-independent. For a real mirror shell or segment, these constants typically have errors and in general are azimuth-dependent. In addition, the mirror segment has additional errors that cannot not fully captured by these three terms. In what follows we will designate these additional errors as the remainder. In other words, a real world segment can be described as

$$\rho(z, \phi) = \rho_0 + \Delta\rho(\phi) + z \cdot \tan[\theta_0 + \Delta\theta(\phi)] - \left(\frac{2z}{L} \right)^2 \cdot [S_0 + \Delta S(\phi)] + R(z, \phi),$$

where each term is described as follows:

1. The parameter ρ_0 is the average radius of the mirror segment, and by definition, is azimuth independent; $\Delta\rho(\phi)$ is radius variation or deviation from circularity, and by definition, is azimuth dependent and has a zero mean.
2. The parameter θ_0 is the average cone angle, and by definition, is azimuth independent; $\Delta\theta(\phi)$ is cone angle variation, and by definition and in general, is azimuth dependent and has a zero mean.
3. The parameter L is the extent of the mirror segment in the Z (or axial) direction).
4. The parameter S_0 is the average sag, and by definition, is azimuth independent; $\Delta S(\phi)$ is the sag variation, and by definition and in general, is azimuth dependent and has a zero mean.
5. The last term, $R(z,\phi)$, includes all the rest of deviation from prescription.

Given the grazing incidence nature of X-ray optics, $R(z,\phi)$'s dependence on azimuth can almost always be neglected without any practical consequence.

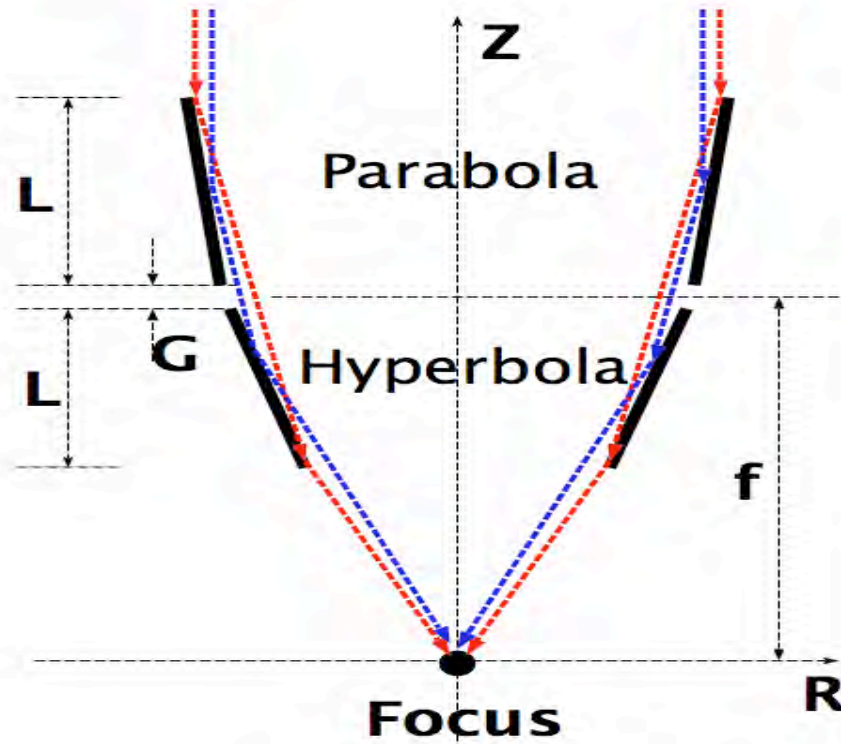


Figure 19. An illustration of a mirror shell.